CALCULATION OF STRESS INTENSITY FACTOR OF CRACKS IN PRESSURE VESSEL USING FINITE ELEMENTS METHOD

SONLU ELEMANLAR METODU KULLANILARAK BASINÇ KABINDAKİ ÇATLAKLARDA STRES YOĞUNLUK FAKTÖRLERİNİN HESAPLANMASI

TUĞÇE GÜZEL

Submitted to
HACETTEPE UNIVERSITY
THE INSTITUTE FOR GRADUATE STUDIES
IN SCIENCE AND ENGINEERING
in partial fulfillment of the requirements for the degree of
MASTER OF SCIENCE
in
NUCLEAR ENGINEERING

2010

CALCULATION OF STRESS INTENSITY FACTOR OF CRACKS IN PRESSURE VESSEL USING FINITE ELEMENTS METHOD

SONLU ELEMANLAR METODU KULLANILARAK BASINÇ KABINDAKİ ÇATLAKLARDA STRES YOĞUNLUK FAKTÖRLERİNİN HESAPLANMASI

TUĞÇE GÜZEL

Submitted to
HACETTEPE UNIVERSITY
THE INSTITUTE FOR GRADUATE STUDIES
IN SCIENCE AND ENGINEERING
in partial fulfillment of the requirements for the degree of
MASTER OF SCIENCE
in
NUCLEAR ENGINEERING

2010

To the Directory of the Institute for Graduate Studies in Science and Engineering,

This study has been accepted as a thesis for the degree of MASTER OF SCIENCE in NUCLEAR ENERGY ENGINEERING by our Examining Committee.

Head: :……
Prof. Dr. Üner Çolak

Advisor :……..
Assoc. Prof. Dr. Bora Yıldırım

Member: :……
Assist. Prof. Dr. Şule Ergün

Member: :……
Assoc. Prof. Dr. Serkan Dağ

Member: :……
Dr. Benat Koçkar

This is to certify that the Board of Directors of the Institute for Graduate Studies in Science and Engineering has approved this thesis on …/…/…..

Prof. Dr. Adil Denizli
Director
The Institute for Graduate Studies in Science and Engineering

CALCULATION OF STRESS INTENSITY FACTOR OF CRACKS IN PRESSURE VESSEL USING FINITE ELEMENTS METHOD

Tuğçe Güzel

ABSTRACT

In this study, finite elements method was used to calculate stress intensity factor of cracks in pressure vessel. The results are obtained by using ANSYS, Inc. which is an engineering simulation software provider. For the analysis, firstly a sample problem is solved to compare the results and prove the accuracy and the code is obtained.

Parameter for initial crack size is defined by Marshall flaw size distribution. Copper and nickel contents, initial reference temperature of the nil-ductility transition, fluence factor, crack-initiation fracture toughness function and arrest fracture toughness functions are treated as inputs from VISA II computer code for predicting the probability of reactor pressure vessel failure which uses NRC reports' parameters.

Keywords: Pressure vessel**,** Stress intensity factor, PTS, Fracture toughness, Finite element method

Advisor: Assoc. Prof. Dr. Bora Yıldırım, Hacettepe University, Department of Mechanical Engineering

Co-advisor: Prof. Dr. Üner Çolak, Hacettepe University, Department of Nuclear Engineering

SONLU ELEMANLAR METODU KULLANILARAK BASINÇ KABINDAKİ ÇATLAKLARDA STRES YOĞUNLUK FAKTÖRLERİNİN HESAPLANMASI

Tuğçe Güzel

ÖZ

Bu çalışmada, basınç kabındaki çatlaklarda stres yoğunluk faktörlerini hesaplamak için sonlu elemanlar metodu kullanılmıştır. Sonuçlar bir mühendislik simülasyon yazılım sağlayıcısı olan ANSYS, Inc. kullanılarak elde edilmiştir. Analiz için, öncelikle sonuçları karşılaştırmak ve doğruluğunu onaylamak amacıyla örnek bir problem çözülmüş ve kod elde edilmiştir.

Başlangıç çatlak boyutu parametresi için Marshall dağılımı tanımlanmıştır. Bakır ve nikel içeriği, sıfır-kırılganlık geçişi başlangıç referans sıcaklığı, doz faktörü, çatlak-başlangıç kırılma tokluğu ve yakalama kırılma tokluğu fonksiyonları reaktör basınç kabı işlevsizleşme olasılığını tahmin etmek için NRC raporlarının parametrelerini kullanan bir bilgisayar kodu olan VISA II kodundan alınmıştır.

Anahtar Sözcükler: Basınç kabı**,** Stres yoğunluk faktörü, PTS, kırılma tokluğu, Sonlu elemanlar metodu K_{Ic} =kırılma tokluğu

Danışman: Doç. Dr. Bora Yıldırım, Hacettepe Üniversitesi, Makine Mühendisliği Bölümü
Yardımcı danışman: Prof. Dr. Üner Çolak, Hacettepe Üniversitesi, Nükleer Enerji Mühendisliği Bölümü

ACKNOWLEDGEMENTS

I would like to thank my advisor Assoc. Prof. Dr. Bora Yıldırım and my co-advisor Prof. Dr. Üner Çolak for their guidance, support and constructive suggestions.

I also want to thank Assist. Prof. Dr. Şule Ergün and Şamil Osman Gürdal, Research Assistant for their valuable comments and contributions. I am grateful for their useful guidance and encouragement.

Finally, I wish to thank my family for supporting me all through this period of study.

Hacettepe University
Department of Nuclear Engineering
September 2010

Table of Contents

LIST OF FIGURES Page

LIST OF TABLE Page

1. INTRODUCTION

In this study, stress intensity factor of currently existing semi elliptical crack in pressure vessel in case of a small break loss of coolant accident is calculated and the stress intensity factor is compared to fracture toughness for crack initiation and crack arrest.

Although there are some analyses in the literature including the calculation of stress intensity factor of semi elliptical crack using finite element methods, there is not any analysis about cracks on reactor pressure vessels under pressurized thermal shock (PTS) condition as performed in this study.

The crack in this study is placed in the weld region of the vessel and the analyses are performed assuming a small break loss of coolant accident. The aim of this thesis is to see the propagation of the possible cracks on pressure vessel. Besides the crack analyses described here, the largest crack investigated is enlarged and crack propagation is examined for this crack.

1.1 Objectives

Pressure vessel which contains reactor core is the most important component of the light water reactors, since it is the most critical barrier against radiation generated in the core. Pressure vessel holds coolant at high temperature and high pressure during operation therefore it is designed and manufactured according to strict regulations. In case of a rupture or leakage in the primary system of a nuclear power plant, the coolant is lost and rapid depressurization occurs in the vessel. This is the design basis accident for a light water reactor and it is called loss-of-coolant accident (LOCA). The results of a LOCA could result in reactor vessel damage. Therefore this may cause release of radioactive substances to the environment.

There are three types of loss-of-coolant accident named after the size of break. These are small break LOCA, medium break LOCA and large break LOCA. In small break loss of coolant accidents the break size would be up to 12cm in diameter and the break would be in the primary circuit.

Each nuclear plant design includes Emergency Core Cooling System (ECCS) specifically to deal with a LOCA since ECCS is designed to inject colder coolant to the vessel to compensate the coolant lost. Sudden cooling of the hot reactor vessel under accidental condition may jeopardize the safety of a pressurized water reactor (PWR). When the reactor pressure vessel is severely overcooled, Pressurized Thermal Shock (PTS) occurs. Pressurized Thermal Shock leads to very high tensile stress in the component which may lead to tearing of the vessel wall under the presence of a small flaw (crack) at the weld region.

In this study, for a currently existing crack in the core region in pressure vessel, stress intensity factor of the crack is calculated using finite element method. Crack is assumed to be in the weld region of the core which is assumed as the heart of the reactor. In case of a crack, leakage of radioactive material may occur. On crack tips of the crack stress intensity factor and fracture toughness for crack initiation and arrest values are obtained and compared to see if the crack propagates or not.

In order to have a complete and comprehensive analysis, the results of the simulations of temperature and pressure history of a small break LOCA are used. The objective of this thesis is to observe if a currently existing crack on vessel propagates or not under small break LOCA conditions. Analyses are performed for different cases of initial crack size and depth to length aspect ratio values.

1.2 Thesis Overview

This thesis includes 5 chapters. The first chapter includes the description of the aim of the thesis and introduction to pressure vessel structure and the brief information on loss of coolant accidents.

Chapter 2 includes the listing of the information on fracture mechanics, stress intensity factor and its three modes, loss of coolant accident (LOCA), pressurized thermal shock (PTS), fracture toughness for crack initiation and arrest, crack initiation and arrest conditions and the cases that the crack propagates.

In Chapter 3, firstly, a test problem that is solved in order to get the crack code in ANSYS is described. Semi elliptical crack is defined on a rectangular geometry, and for two cases of a/c (crack depth versus crack length aspect ratio) analyses are performed and results are compared [1]. So that the code obtained from study of Yıldırım et al. is tested. According to the results, it is seen that the code works correctly when finite element method is applied. Then in the second part of Chapter 3, the description of the analyses to be performed is listed. Thermal and pressure analyses performed are summarized. Using SBLOCA temperature history in a 2D axisymetric geometry, thermal analysis is performed applying convection on one side and assuming heat flux as zero on other sides. Using the temperature values obtained, a temperature equation to be used as input in the code is obtained. In addition the pressure history of SBLOCA, parameter for initial crack size defined by Marshall flaw size distribution, copper and nickel contents, initial reference temperature of the nil-ductility transition, fluence factor are other inputs for the code.

In Chapter 4 the results of the analysis are given. Toughness and stress intensity values obtained from the code are plotted. Temperature values of the crack tip are also presented. Fracture toughness for crack initiation and arrest values are compared to stress intensity values to observe crack propagation. In Chapter 5, results are summarized and conclusions are presented.

2. FRACTURE MECHANICS

In this chapter brief information on structures of cracks simulated in this study and the LOCA through which crack propagation is given.

2.1 Fatigue and Fracture

Study of cracks, how they form and how they grow due to cyclic stress is called fatigue. It is the progressive and localized structural damage that occurs when a material is subjected to cyclic loading.

Fracture is the local separation of an object or material into two or more pieces under the action of stress. A fracture may reduce strength or inhibits transmission of light, depending on substance. If the potential energy released as the crack grows is greater than the energy needed to create new crack surface, then the material will fracture.

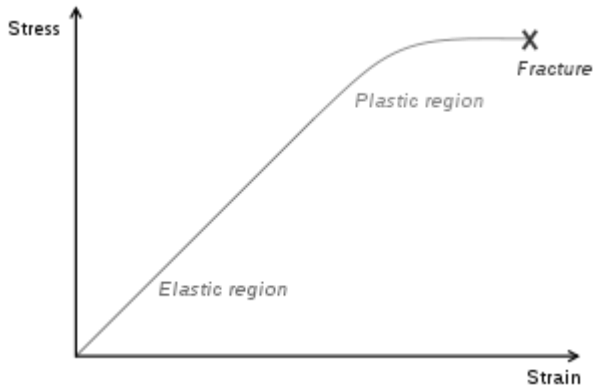

Figure 2. 1 Diagram of Stress-strain curve

Figure 2.1 shows the relationship between stress (force applied) and strain (deformation) of a ductile metal.

In materials science, fracture toughness is a property which describes the ability of a material containing a crack to resist fracture, and is one of the most important properties of any material for virtually all design applications. It is denoted K_{Ic} and has the units of Pa$\sqrt{m}$.

The subscript 'Ic' denotes mode I crack opening under a normal tensile stress perpendicular to the crack, since the material can be made thick enough to resist shear (mode II) or tear (mode III).

Fracture toughness is a quantitative way of expressing a material's resistance to brittle fracture when a crack is present. If a material has a large value of fracture toughness it will probably undergo ductile fracture. Brittle fracture is very characteristic of materials with a low fracture toughness value.

Fracture mechanics is the field of mechanics concerned with the study of the formation of cracks in materials. It uses methods of analytical solid mechanics to calculate the driving force on a crack and those of experimental solid mechanics to characterize the material's resistance to fracture.

2.2 Stress Intensity Factor

Stress Intensity Factor, which is denoted as K, is used in fracture mechanics to more accurately predict the stress state (stress intensity) near the tip of a crack caused by a remote load or residual stresses. It is a theoretical construct applicable to a homogenous elastic material. It is a useful for providing a failure criterion for brittle materials.

The magnitude of stress intensity factor depends on many parameters such as sample geometry, the size and location of the crack, and the magnitude and the modal distribution of loads on the material.

$$K = Y\sigma\sqrt{\pi a} \qquad (2.1)$$

Y = function of specimen and crack geometry (dimensionless)

σ = applied stress

a = crack length

Stress Intensity is a parameter that amplifies the magnitude of the applied stress which includes load type as geometrical parameter. According to these load

types there are three modes of stress intensity factor which are Mode-I, Mode-II or Mode-III.

- *Mode I crack* – This is the opening mode of a crack (in which a tensile stress normal to the plane of the crack) (also the most common type is Mode-I)
- *Mode II crack* – This is the sliding mode (in which a shear stress acting parallel to the plane of the crack and perpendicular to the crack front)
- *Mode III crack* – This type is the tearing mode (in which a shear stress acting parallel to the plane of the crack and parallel to the crack front)

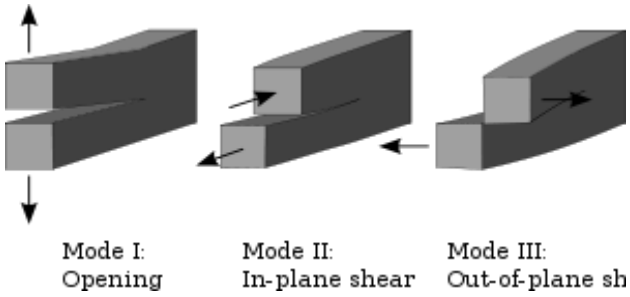

Figure 2. 2 Three modes of stress intensity factor

Mode-I is opening or tensile mode where the crack surfaces move apart. Mode-II is sliding or in-plane shear mode where the crack surfaces slide one over another in a perpendicular direction to the leading edge of the crack. Mode-III is tearing and antiplane shear mode where the crack surfaces move relative to one another and parallel to the leading edge of the crack.

Stress Intensity in any mode situation is directly proportional to the applied load on the material. If the crack in a material is very sharp, the minimum value of K_I can be empirically determined, which is the critical value of stress intensity required to propagate the crack. This critical value determined for Mode-I loading in plane-strain is referred to as the critical fracture toughness, which is denoted as K_{IC}, of the material. K_{IC} has units of stress times the root of a distance. The units of K_{IC} infer that the fracture stress of the material must be reached over

some critical distance in order for K_{IC} to be reached and crack propagation to occur.

The stress intensity, K_I, represents the level of “stress” at the tip of the crack and the fracture toughness, K_{IC}, is the highest value of stress intensity that a material under very specific (plane-strain) conditions that a material can withstand without fracture. As the stress intensity factor reaches the K_{IC} value, unstable fracture occurs. As with a material’s other mechanical properties, K_{IC} is the most often used engineering design parameter in fracture mechanics and hence must be understood if we are to design fracture tolerant materials. Typically for most materials if a crack can be seen it is very close to the critical stress state predicted by the Stress Intensity Factor.

2.3 Loss of Coolant Accident (LOCA)

A loss of coolant accident (LOCA) is a mode of failure for a nuclear reactor; if not managed effectively, the results of a LOCA could result in reactor core damage. Loss of coolant accident occupies a central position in the safety analyses of light-water-cooled reactor. The high-pressure and high-temperature water represents a large inventory of stored energy that may be released over a short period of time in case of a LOCA.

Nuclear reactors generate heat internally; to remove this heat and convert it into useful electrical power, a coolant system is used. If this coolant flow is reduced, or lost altogether, the nuclear reactor's emergency shutdown system is designed to stop the fission chain reaction. However, due to radioactive decay the nuclear fuel will continue to generate a significant amount of heat.

When loss of coolant accident occurs, emergency core cooling system is driven in to prevent the system from high temperature. If emergency core cooling system does not drive in, this will cause system temperature to increase and this may cause core meltdown.

If a break occurs in the hot leg of the primary coolant loop [3], emergency core cooling system drives in. The temperature starts to decrease rapidly with cold water injection. The coolant flow rate through the break is greater than the charging and emergency core cooling flow rate, this causes system pressure to decrease.

There are three types of loss of coolant accident named according to the size of the break. These are Small Break LOCA, Medium Break LOCA and large break LOCA. When the break is up to 12 cm in diameter, this type of LOCA is called Small Break LOCA (SBLOCA). Although Large Break LOCA is the limiting case, depending on the higher probability of occurrence of SBLOCA, the analyses are performed using the results of small break LOCA simulations in this study.

The temperature and pressure histories of LOCA events are presented in Figures 2.3 and 2.4.

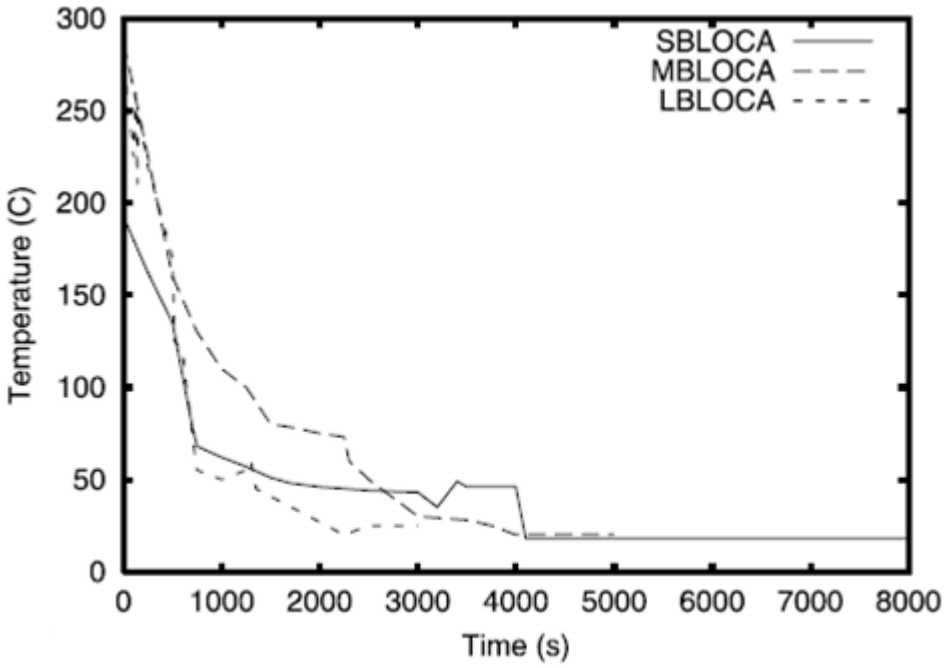

Figure 2. 3 Temperature history of LOCA events [3]

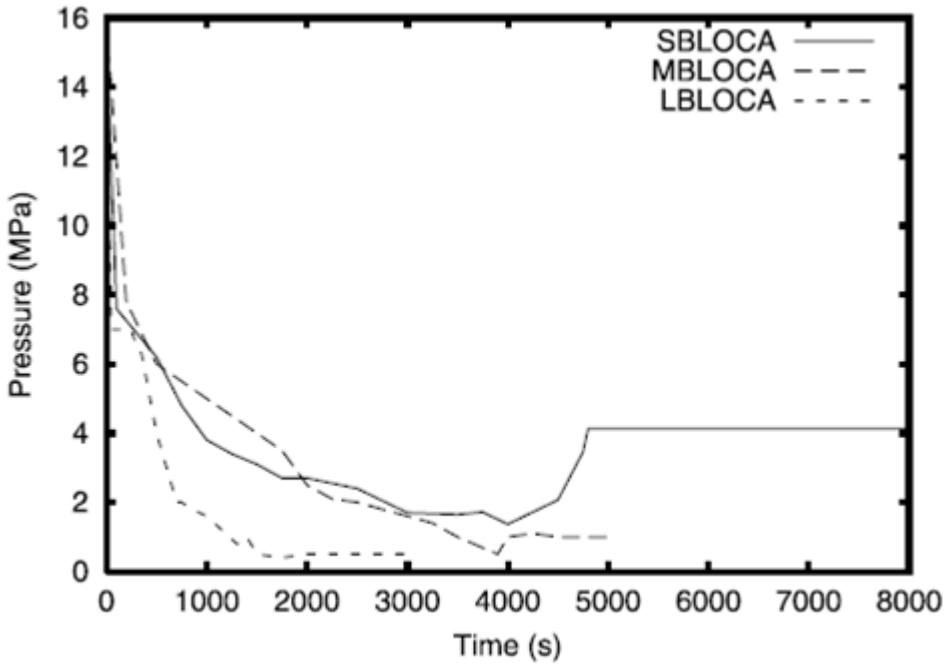

Figure 2. 4 Pressure history of LOCA events [3]

These figures will be used in thermal and pressure analysis as will be explained in analysis chapter 4.

2.4 Pressurized Thermal Shock (PTS)

One of the most severe transients which may jeopardize the safety of a pressurized water reactor (PWR) is the sudden cooling of the hot reactor vessel under accidental condition. This phenomenon is commonly known as pressurized thermal shock (PTS).

During the operation of a nuclear power plant, the reactor pressure vessel (RPV) walls are exposed to neutron radiation, resulting in localized embrittlement of the vessel steel and weld materials in the area of the reactor core. If an embrittled reactor pressure vessel had an existing flaw of critical size and certain severe system transients were to occur, the flaw could propagate very rapidly through the vessel, resulting in a through-wall crack and challenging the integrity of the reactor pressure vessel. The severe transients of concern, known as pressurized thermal shock (PTS), are characterized by a rapid cooling (i.e., thermal shock) of the internal RPV surface and downcomer, which may be followed by repressurization of the RPV. Thus, a PTS event poses a potentially significant challenge to the structural integrity of the RPV in a pressurized-water reactor (PWR).

A number of abnormal events and postulated accidents have the potential to thermally shock the vessel (either with or without significant internal pressure). These events include a pipe break or stuck-open valve in the primary pressure circuit, a break of the main steam line, etc. During such events, the water level in the core drops as a result of the contraction produced by rapid depressurization. In events involving a break in the primary pressure circuit, an additional drop in water level occurs as a result of leakage from the break. Automatic systems and operators must provide makeup water in the primary system to prevent overheating of the fuel in the core. However, the makeup water is much colder than that held in the primary system. As a result, the temperature drop produced by rapid depressurization coupled with the near-ambient temperature of the makeup water produces significant thermal stresses in the thick section steel wall of the RPV. For embrittled RPVs, these stresses could be sufficient to initiate a running crack, which could propagate all the way through the vessel wall. Such

through-wall cracking of the RPV could precipitate core damage or, in rare cases, a large early release of radioactive material to the environment. Fortunately, the coincident occurrence of critical-size flaws, embrittled vessel steel and weld material, and a severe PTS transient is a very low-probability event. In fact, only a few currently operating PWRs are projected to closely approach the current statutory limit on the level of embrittlement during their planned operational life.

As explained above, consequent to the emergency core cooling injection, pressurized water reactors are subjected to severe thermal shock as a result of rapid cooling of the inner surface of the vessel wall. Analyses of this event indicate that as a result of large tensile stresses developed from pressurized thermal shock (PTS) together with radiation induced embrittlement over the service may lead to rapid propagation of pre-existent flaws.

Due to variation of material properties including hardening modulus and fracture toughness arising from spatial temperature gradient, the elasto-plastic analysis of the vessel becomes time consuming. Hence, the crack initiation as well as arrest conditions is generally assumed in terms of static properties. Most of the studies carried out so far have adopted linear elastic fracture mechanics (LEFM) static procedure. This simpler procedure is satisfactory despite the experimental observations wherein crack initiation takes place when K_I higher than K_{Ic} after some blunting of the crack tip, the resulting crack jump being large.

Fig.2.5 shows a typical temperature, resultant thermal stress, static fracture toughness K_{Ic} and static arrest toughness K_{Ia} distribution in the wall of a vessel at a particular instant in the PTS transient and stress intensity factor values K_I for axial crack of different depths. As a result of steep temperature gradient, fracture toughness K_{Ic} also rises steeply with depth; however as K_I also increases with depth, both shallow and deep flaw may initiate ($K_I = K_{Ic}$) and then arrest ($K_I = K_{Ia}$) for the case shown. The arrest occurs despite $dK_I/d(a/W) > 0$; though in tests measuring K_{Ia} usually $dK_{Ia}/d(a/W) < 0$: On the basis of static initiation and arrest conditions, the resulting crack extension is a series of initiation arrest sequence shown in Fig. 2.6.

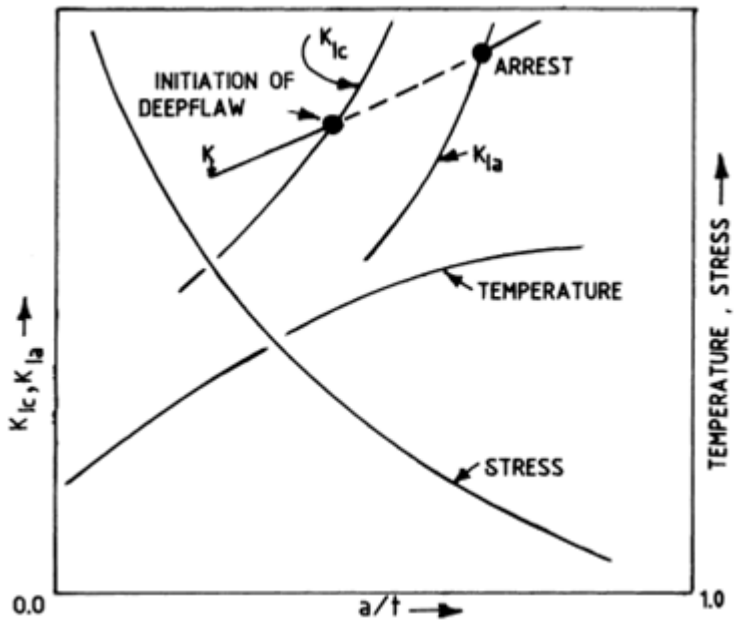

Figure 2. 5 Distribution of various fracture mechanics related parameters across the vessel wall in a PTS transient [13]

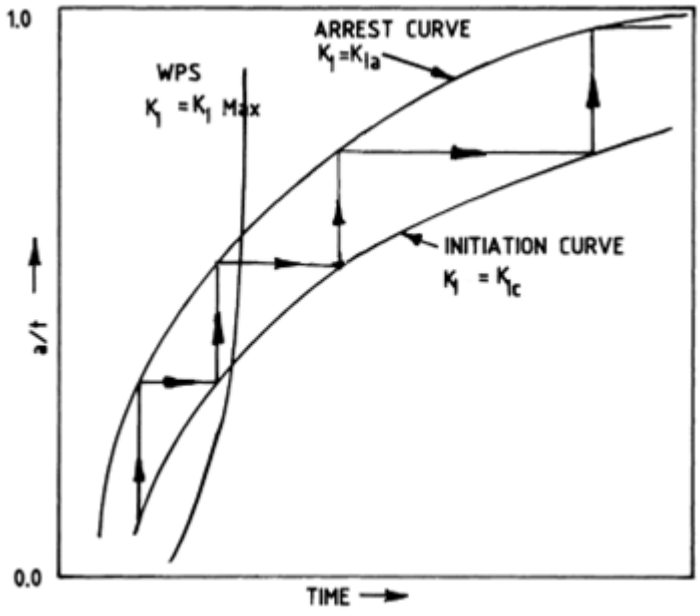

Figure 2. 6 Crack initiation and arrest in a typical PTS transient [13]

This figure also shows the locus of points for $K_I=(K_I)$max; i.e. $dK_I/dt = 0$; a curve commonly referred to as the warm prestress (WPS) curve. For times less than those indicated by WPS curve, K_I increases with time while for times greater than those indicated by WPS curve K_I decreases with time. Under these latter

conditions, a crack could not initiate even with $K_I >> K_{Ic}$. As shown in Fig. 2.6. WPS limits the crack propagation and allows $K_I/K_{Ic}>>1$ for final crack depth during a PTS event.

When the stress intensity factor becomes more than fracture toughness for crack initiation, the crack growth or extension will occur and crack arrest will depend on fracture toughness for crack arrest.

3. PROBLEM DESCRIPTION

In this chapter the checked accuracy of the code to calculate stress intensity factor of semi elliptical crack is described. In order to see whether the results of the code are acceptable or not, the stress intensity values calculated for a semi elliptical crack [1] are compared to the results of the code that will be used for crack analysis in pressure vessel which is the main concern of this thesis.

3.1 Test Problem

The geometry of the semi-elliptical surface crack in a homogeneous block is analyzed. There is a semi-elliptical crack of length 2*c* and depth *a* at the surface x=0, as presented in Figure 3.1.

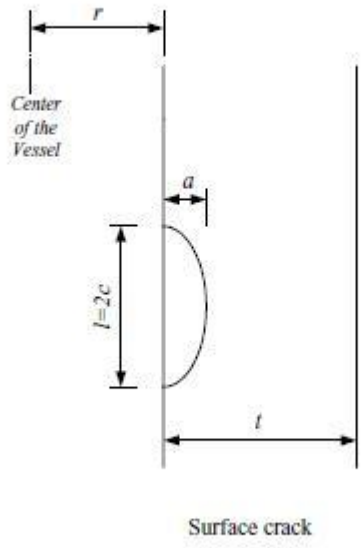

Figure 3. 1 Semi elliptical crack

In the study of Yıldırım et al., besides FGM coating fracture analyses, stress intensity factor for semi elliptical crack is calculated. In this article stress intensity factor for two cases of a/c and a/h ratios are calculated. The results of this article are used to check the accuracy of the crack code obtained for this study that will be used for calculating and comparing stress intensity factor and fracture toughness of crack on pressure vessel. The critical parameters that have to be

considered to obtain convergent results are the mesh density and number and size of the elements near the crack front. The crack is placed in a rectangular block and the stress intensity factor is calculated using Von Misses Stresses.

To calculate stress intensity;

$$Q = \begin{Bmatrix} 1+1.464(a/c)^{1.65} & \text{for} & (a/c) \le 1 \\ 1+1.464(c/a)^{1.65} & \text{for} & (a/c) > 1 \end{Bmatrix} \qquad (3.1)$$

Q is a function of aspect ratio a/c

a/c is crack depth versus crack length aspect ratio,

$$K_{In} = \frac{\mathrm{K_I}}{\sigma_{\mathrm{t}} \sqrt{\pi a / Q}} \qquad (3.2)$$

σ_t is the uniform tension

The analysis is performed for two different a/c ratios, 2 and 1/3, respectively [1].

3.1.1 Analysis for the Case a/c=2

The half of the crack presented on Figure 3.2 is modeled on a plate and symmetric boundary conditions are applied. The angle seen on Figure 3.2 is taken from 0 to π/2.

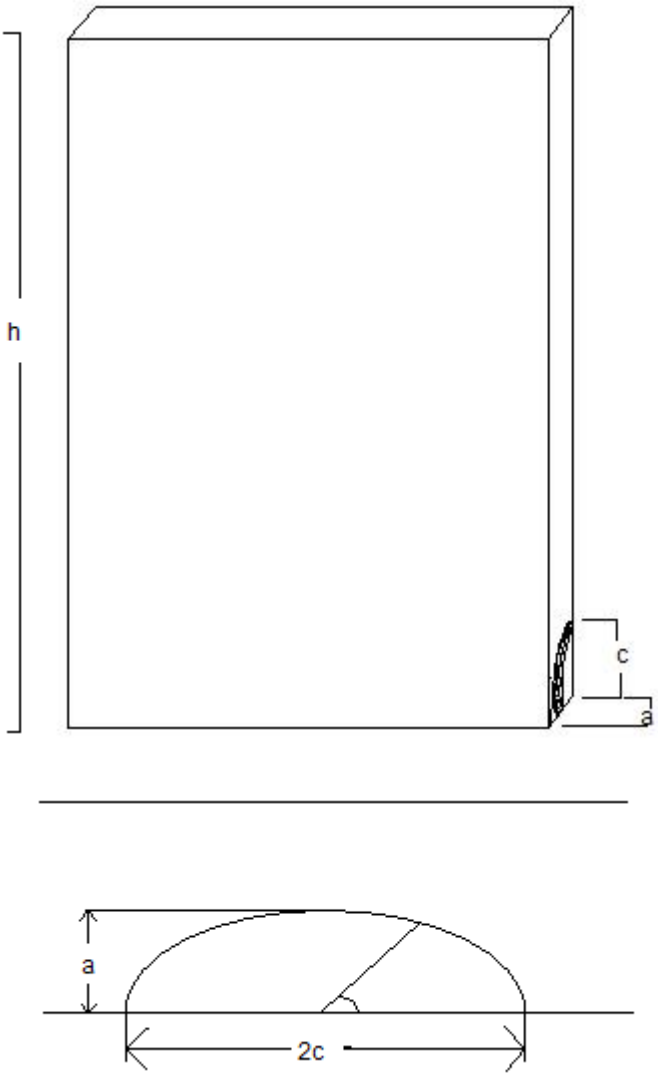

Figure 3.2 Depth (a) and length (c) of the crack and parametric angle ϕ is shown in the crack geometry above.

Parameters used in the analysis are
Modulus of elasticity = 1 MPa
Poisson's ratio = 0.25

Figure 3.3 (a) and Figure 3.4 (a) show the geometry of the problem, when crack depth versus crack length aspect ratio (a/c) is 2 and 1/3, respectively. The plots

shown in Figure 3.3 (b) and Figure 3.4 (b) represent the comparison of the results for present study and the reference study.

For a/c =2 case, in order to have an infinite geometry, dimensions are taken as h, 20h, 20h

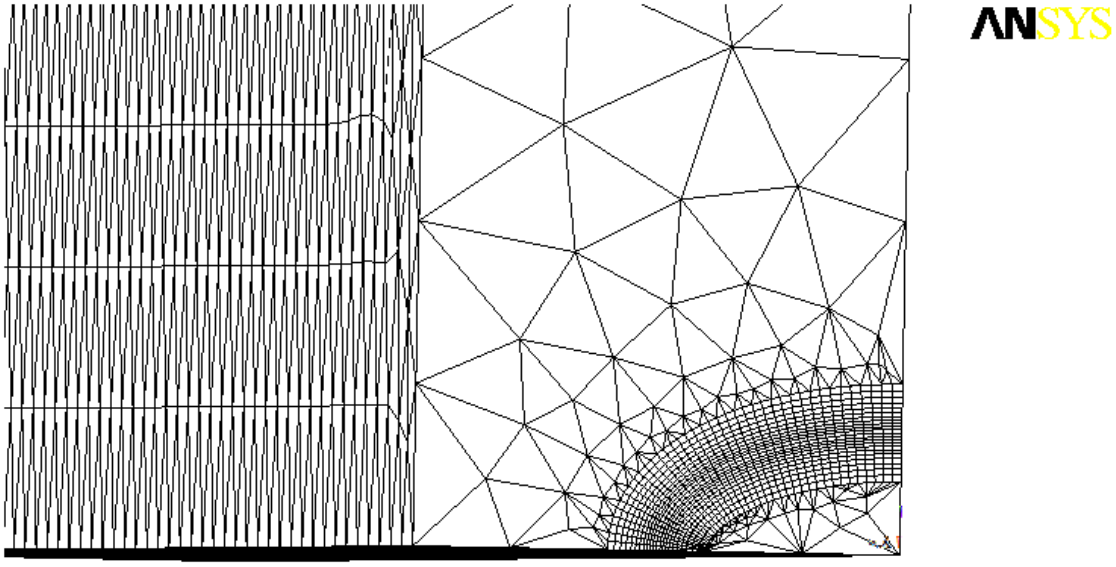

Figure 3.3 (a) Geometry for a/c =2

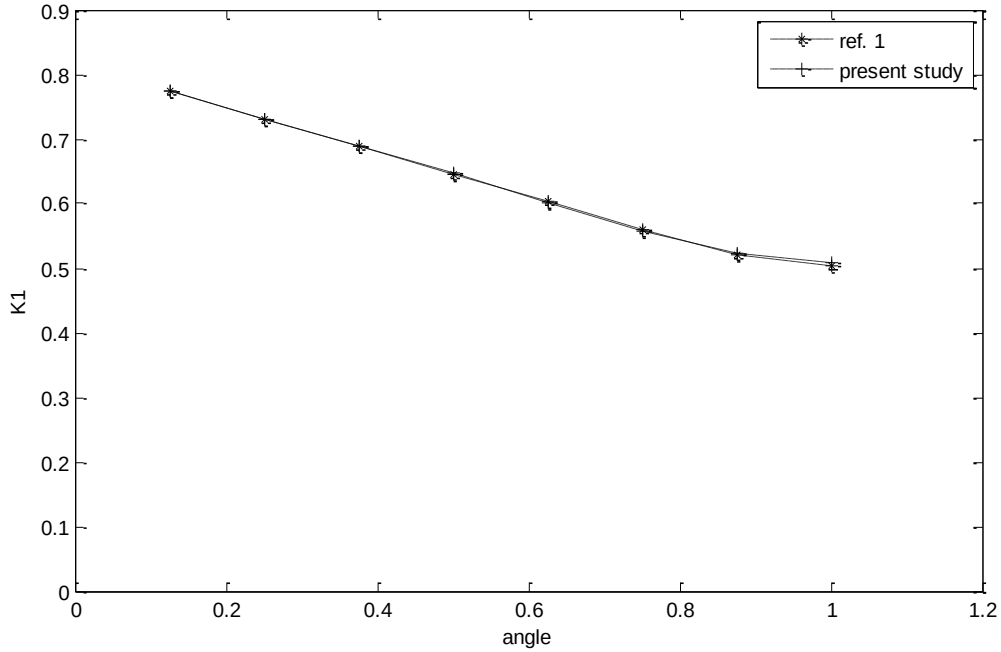

Figure 3.3 (b) Results for a/c = 2

3.1.2. Analysis for the Case a/c=1/3

For a/c =1/3 case, dimensions are taken as h, 20h and 20h.

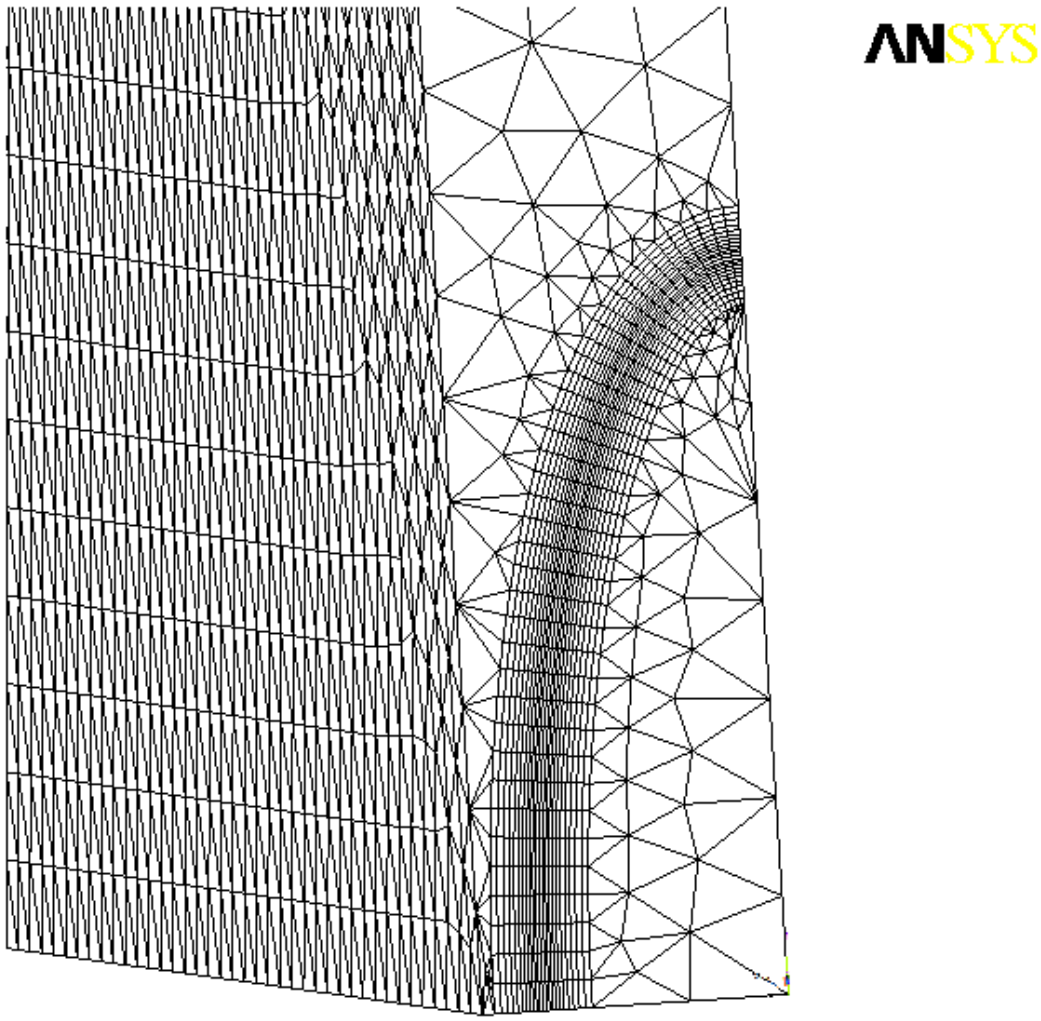

Figure 3.4 (a) Geometry for a/c = 1/3

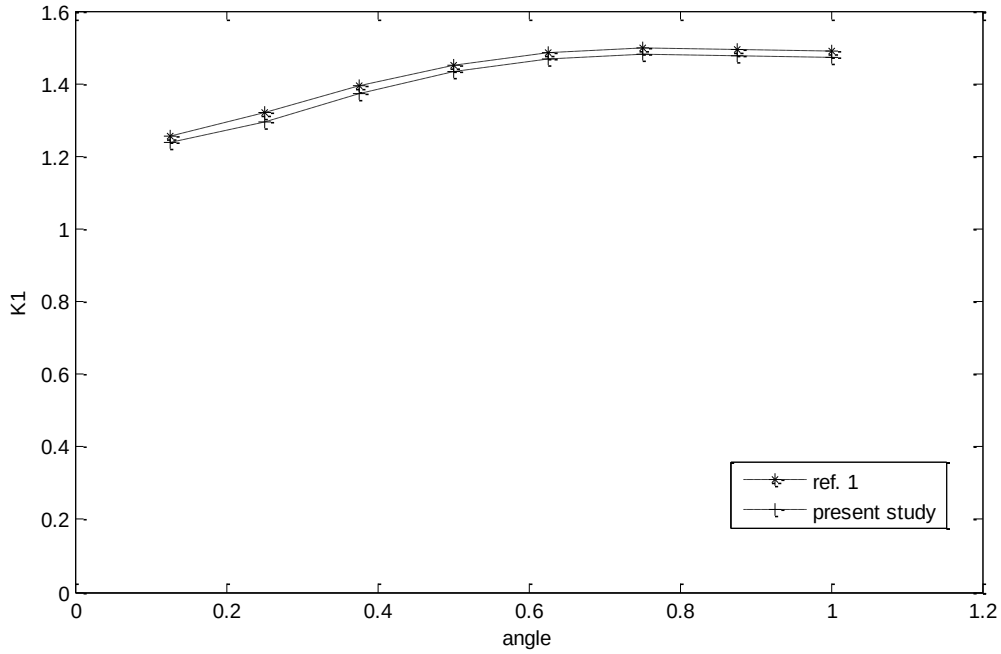

Figure 3.4 (b) Results for a/c = 1/3.

Comparisons of the normalized mode I stress intensity factors K_{In} for a homogeneous plate subjected to uniform tension σ_t, v=0.25, $E(h)/E1$=1 are given in Table 3.1.

Table 3. 1 Comparison of the normalized mode-I SIF

$2\varphi/\pi$	a/h=0.5, a/c=2	Present Study	a/h=0.8, a/c=1/3	Present study
0.125	0.774	0.7754	1.255	1.240
0.250	0.731	0.7300	1.321	1.293
0.375	0.689	0.6894	1.395	1.372
0.500	0.646	0.6468	1.452	1.435
0.625	0.603	0.6018	1.487	1.469
0.750	0.560	0.5573	1.498	1.480
0.875	0.521	0.5221	1.495	1.478
1.000	0.504	0.5074	1.490	1.474

Table 3.1 indicates that the results of the reference study and the code obtained in this study are in good agreement.

Comparisons of results are also shown in Figure 3.3 (b) and Figure 3.4 (b). The maximum error is almost 1% and the acceptable error is 3%. As a result it is decided that the code for the crack is obtained correctly and this code is used to simulate the crack at the reactor pressure vessel. New analyses are performed for PWR pressure vessel fabricated by using SA533B type ferritic steel.

3.2 Description of the Modeled Problem

In this section, the problem analyzed and the details of the modeling are described. Since the calculations performed in the study requires information on pressure and temperature history of SBLOCA. It is also described in this section.

3.2.1 Pressure Vessel

The pressurized water reactor (PWR) has a compact core and a high system pressure therefore its vessel has thick walls. The system pressure in a PWR is kept at approximately 15.5 MPa.

The vessel contains the reactor core and core structure, control rods with guide tubes and instrumentation. The vessel structure mainly consists of an upper and a lower support structure, the core barrel and the thermal shield. The upper core support structure acts as a support for the upper ends of the fuel assemblies. It protects and guides the control rods. The lower core support structure carries the core, the core barrel and the thermal shield. The core barrel separates the core from the down comer space near to the vessel wall. The thermal shield provides shielding from core radiation. Thermal shield also reduces irradiation damage and thermal stress in the pressure vessel wall. Reactor vessel and connected coolant loops generate the reactor coolant system. The coolant enters the reactor vessel through the inlet nozzles and flows upward on both sides of the thermal shield which is located in the down comer between the core barrel and the reactor vessel. The drawings of reactor vessel are presented in Figure 3.5.

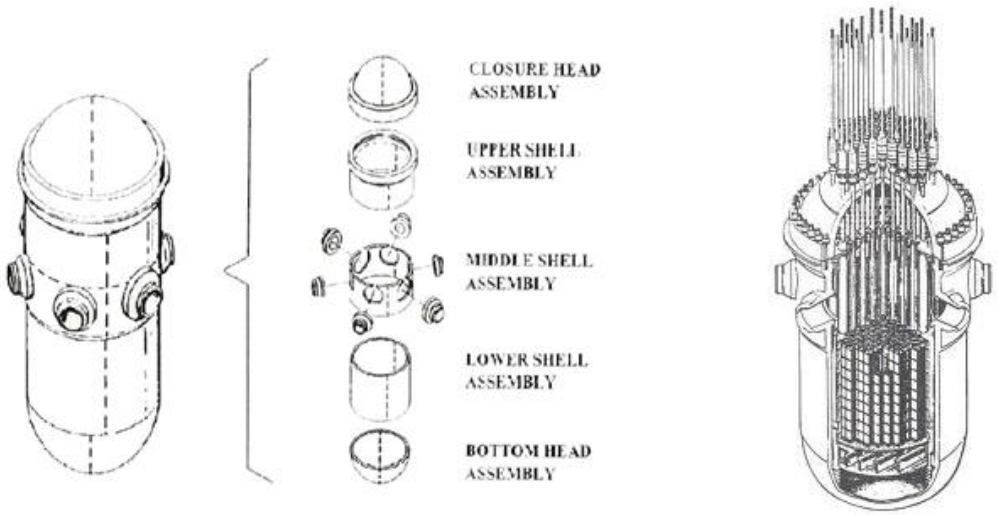

Figure 3.5 An expanded view and a closer view of pressure vessel

Pressure vessels are subjected to thermal and mechanical loads during normal and abnormal operating conditions and transients. Therefore, the reactor vessel faces different problems during its service life.

The vessel walls in the reactor beltline region are subjected to the highest fluence and degradation due to irradiation embrittlement. Therefore, the welds within that region become possibly the weakest link since the welds are likely to contain defects that can become cracks. Welds are of primary concern in pressure vessel integrity analysis. The major variables depending on weld parameters in this study are copper and nickel contents [6].

Two types of materials are used to manufacture most of light water reactor vessels; SA533B-1 and SA508-2. In this study SA533B-1 type steel is modeled. Pressure vessel steels are manufactured by taking the fracture toughness, yield strength and the irradiation embrittlement properties of material into account. The resistance of a material to crack extension is known as fracture toughness. Pressure vessel steel is characterized by high fracture toughness. Fracture toughness also depends on structure temperature.

Figure 3.6 shows cross section of the reactor core. Reactor vessel inner wall is almost 0.5m far away from the core.

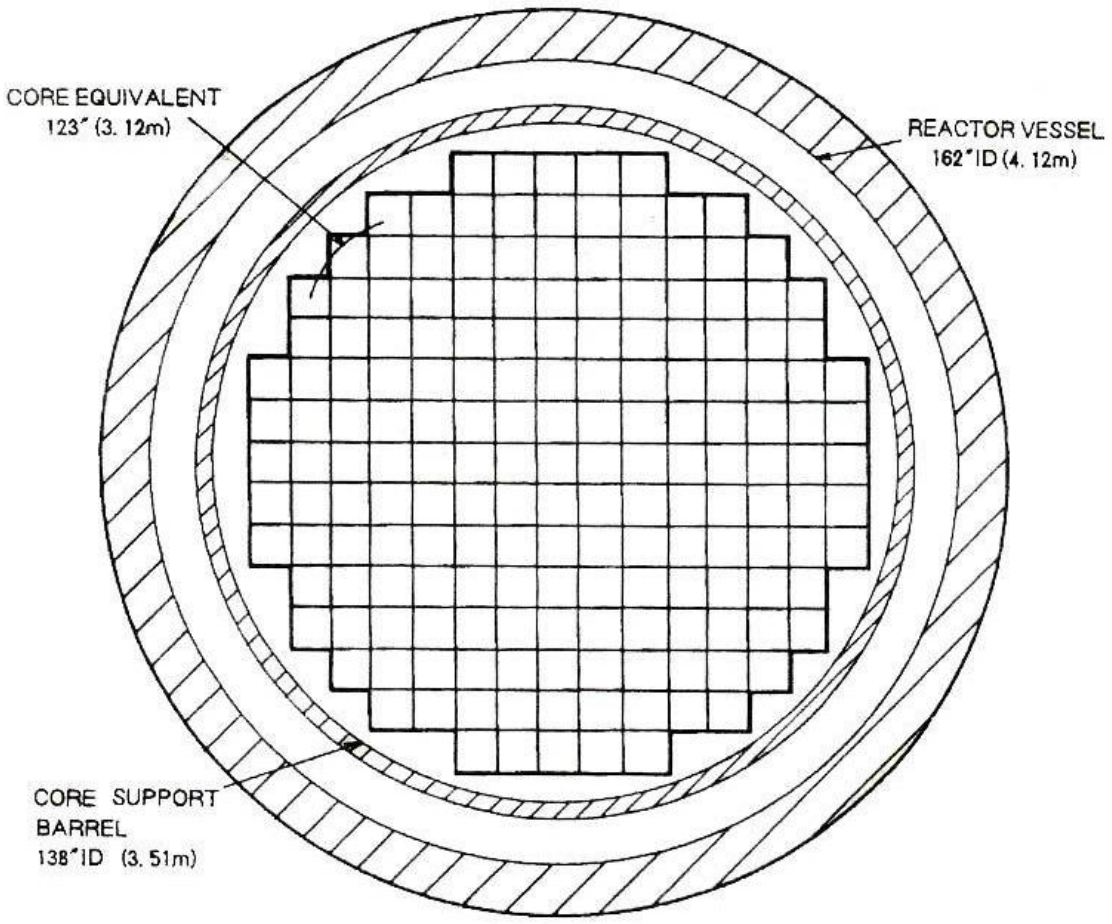

Figure 3.6 Reactor core cross-section

3.2.2 Thermal Analysis

For the analysis the crack propagation is modeled under SBLOCA conditions as described in Chapter 2. To obtain the temperature distribution through the pressure vessel wall, temperature history of SBLOCA analysis that is shown in Figure 2.3 is used. This temperature history is applied on the inner wall of the pressure vessel. The temperature values in the pressure vessel wall are obtained by thermal analysis to derive the temperature equation, which is a function of location and time.

Firstly using the temperature results of a small break loss of coolant accident in a reactor pressure vessel, thermal analysis is done. For the thermal analysis, density and specific heat values and the vessel properties presented in Tables 3.2 and 3.3 are used [2],[3].

Table 3. 2 PWR pressure vessel characteristics [2]

PWR pressure vessel characteristics	
Overall height	13 660 mm
Inside diameter	4394 mm
Wall thickness	215 mm
Normal operating pressure	15.98 MPa
Initial temperature	300 ^{0}C

Table 3. 3 Properties of vessel [3]

Properties of vessel	
Modulus of elasticity, E	195.5 GPa
Poisson's ratio	0.3
Thermal conductivity, k	39.4 W/m K
Specific heat capacity, C_p	700 J/kg K
Density of steel	7800 kg/m^3
Thermal expansion coefficient ($10^{-6}K^{-1}$)	12.4

For 3000 seconds SBLOCA transient analysis is performed assuming 2D axisymmetric conditions. Thermal conductivity, density, specific heat capacity values are from Table 3.3 and convection value is taken as 1703.478 W/m^{2}K. The dimensions of the geometry are r1=2.197m, r2=2.412m, h= 2m. For all boundaries heat flux is taken as 0 and on one side, convection is applied. This assumption is based on the absence of the cooling water flaw on three sides of the vessel. And the temperature values taken from SBLOCA [3] are applied to the inner surface.

The results of transient analysis are obtained assuming a path. Using these values an equation to be used in crack analysis on pressure vessel is derived for temperature as a function of position and time. This equation gives us the temperature distribution in pressure vessel along 22 cm thickness.

3.2.3 Pressure Analysis

Pressure values of small break loss of coolant accident are taken from the analysis done in the literature [3]. Once the pressure values are obtained they are fitted to an equation. Figure 3.7 shows the SBLOCA pressure history [3] and the pressure change used in this study. It is seen that the error between the obtained pressures can be ignored. Pressure distribution is applied to the inner surface of the pressure vessel.

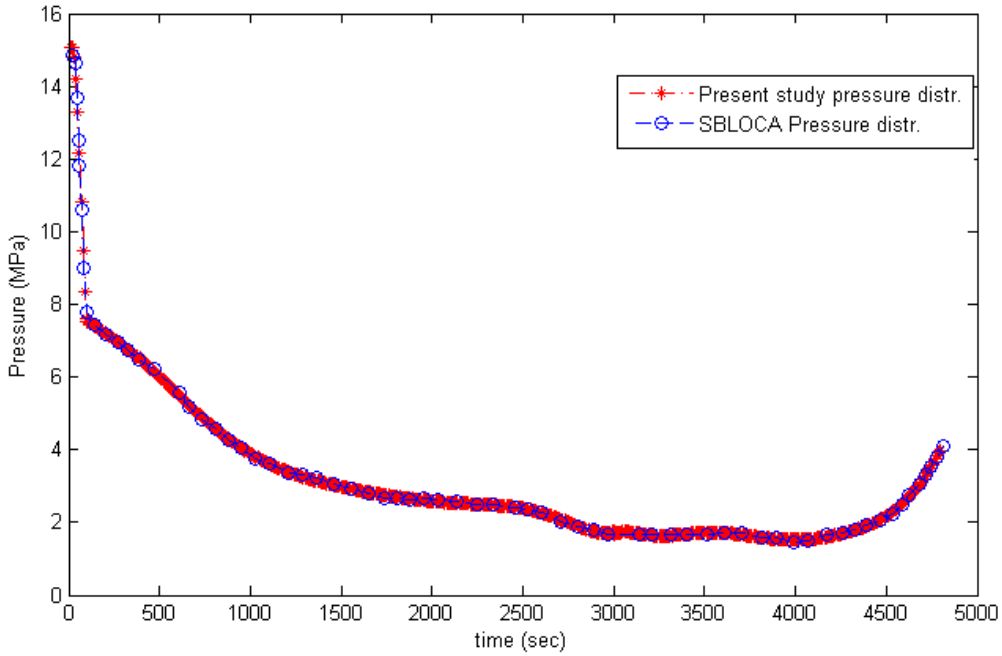

Figure 3.7 Pressure History for Small Break Loss of Coolant Accident

3.2.4. Description of the Analysis Performed

The flaw distribution in the crack is obtained from Marshall distribution. The Marshall distribution is used in vessel failure probability analyses. The probability of crack on pressure vessel is very small, almost 10^{-6} according to Reactor Safety Study (WASH-1400). The equation for Marshall distribution function is: [8]

$$f(x) = 0.034e^{-4.06x} + 6.88e^{-6.94x} \qquad (3.3)$$

Copper and nickel contents are taken as 0.117 and 0.547, respectively.

In this study, stress intensity factor of cracks in pressure vessel is calculated using finite element method. For this analysis, 7 different crack lengths, which are shown in Table 3.4, are obtained using Marshall distribution.

Table 3. 4 Marshall distribution

Pa from Marshall Distribution	A (cm)
0.72614885	0.039
0.06946752	0.044
0.00562507	0.134
0.00021033	0.252
0.00001118	0.357
0.00000096	0.445
0.00000011	0.522

For the biggest crack length, 0.522 cm, different a/c ratios are analyzed. These are a/c= 1/2, 1/3, 1/4, 1/5. The crack propagation is observed.

Initial temperature for the analysis is taken as 300 °C.

Reference temperature calculation is done [10] and the formulation for the reference temperature is

$$RT_{NDT} = RT_{NDT0} + M + \Delta RT_{NDT} \qquad (3.4)$$

$$RT_{NDT0} = \text{ - } 6.65\ ^{0}C\ \ (20F)$$

$M = 2\sqrt{\sigma_u^{\,2} + \sigma_\Delta^{\,2}}$ which is approximately 59 F

$\sigma_u = 17F$ and $\sigma_\Delta = 24F$ (taken as constant values [8])

$$\Delta RT_{NDT} = (CF)\, f^{(0.28 - 0.10 \log f)}$$

To calculate ΔRT_{NDT} Copper and Nickel contents given above are needed. CF, which is the abbreviation for chemistry factor [10] as 125.18 and f which is a function of irradiation is taken from flux 4 x 10^{19}n/cm^2 as 4 [3]. f is the fluence

factor and it decreases exponentially. The value of f used in this analysis is the maximum value.

The temperature equation lets us to get the temperature value in every point from radius 1 to radius 2. To calculate fracture toughness value at a and c points of the crack, following equations are used.

$$K_{Ic} = \begin{cases} 36.2 + 49.4e^{0.0104(T - RT_{NDT})} & , \quad T - RT_{NDT} \le 50 \\ 55.1 + 28e^{0.0214(T - RT_{NDT})} & , \quad T - RT_{NDT} > 50 \end{cases} \qquad (3.5)$$

K_{Ic} is the fracture toughness for crack initiation
T is the temperature value on nodes
RT_{NDT} is ductile to brittle transition temperature and calculated as explained above

$$K_{Ia} = \begin{cases} 19.9 + 43.9e^{0.00993(T - RT_{NDT})} & , \quad T - RT_{NDT} \le 50 \\ 70.1 + 6.50e^{0.0196(T - RT_{NDT})} & , \quad T - RT_{NDT} > 50 \end{cases} \qquad (3.6)$$

K_{Ia} is the fracture toughness for crack arrest
T is the temperature value on nodes
RT_{NDT} is ductile to brittle transition temperature and calculated as explained above

As can be seen from above equations the toughness depends on the temperature and the transition temperature given by RT_{NDT} temperature.

Figure 3.8 shows the crack geometry modeled.

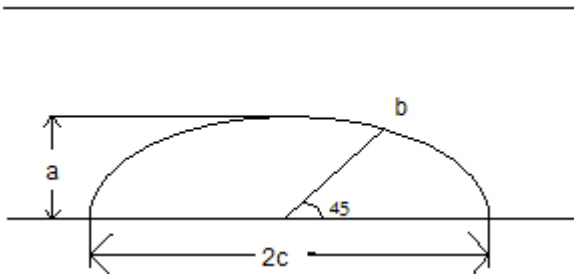

Figure 3.8 Crack geometry

The stress intensity values at points a (see Figure 3.8) (K_A) and c (see Figure 3.8) (K_C) are compared to the values of crack arrest at point a (K_{IAA}) and point c (K_{IAC}). If arrest values are smaller than stress intensity values, it means the crack

can propagate. In this study, the cases in which crack propagation can occur are analyzed.

When stress intensity factor exceeds fracture toughness for crack initiation, the crack growth is estimated at the current crack front nodes based on the difference between K_I^2 and K_{IA}^2. The crack front nodes are shifted by a/10 and depending on K_I^2 and K_{IA}^2 for a and c, respectively. The new K_I values are computed and compared with K_{IA}. The crack growth is recalculated and supplied to the model. The procedure is repeated till the computed K_I along the crack front is almost equal to K_{IA}. The crack growth and arrest analysis is repeated at the next time step.

4. ANALYSIS AND RESULTS

In this chapter, the analyses for seven different crack sizes, which are obtained from Marshall Distribution, are performed and the biggest initial crack is enlarged to observe the propagation for different a over c values. Toughness and stress intensity values obtained from the code are plotted. Fracture toughness for crack initiation and arrest values are compared to stress intensity values. Temperature values of the crack tip are also presented. Finally, all the results are given on tables.

4.1 Analysis

In the first part, for the following crack lengths for an elliptical crack, a/c is taken as 1. A quarter of the crack is placed in the dimensions of a common pressure vessel. The weld region is the most dangerous part. So the crack is assumed in the weld region. The weld is assumed to be at the core region part of the vessel. Symmetric boundary conditions are used. To get pressure and temperature values, pressure and temperature equations obtained above are inserted to the code, so that for all distances from inner radius to the outer radius of the pressure vessel, the temperature and pressure values can be obtained.

Stress intensity values and fracture toughness values for crack initiation and arrest in points a and c are calculated.

In Figures 4.1, 4.2 and 4.3 geometry of the pressure vessel and the meshed crack used in the geometry are shown, respectively.

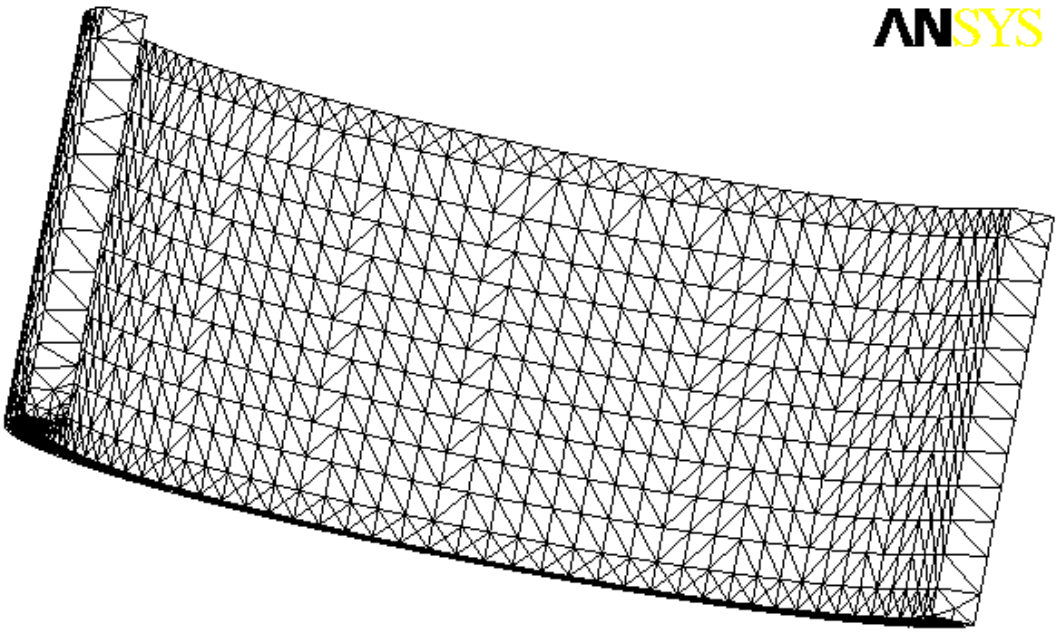

Figure 4.1Pressure vessel geometry

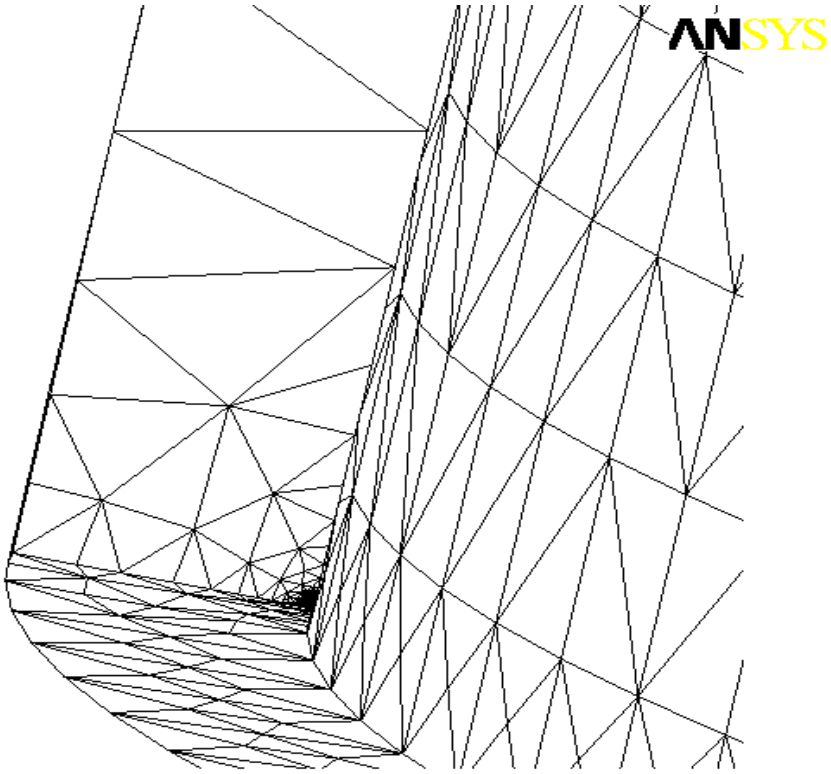

Figure 4.2 Crack on pressure vessel

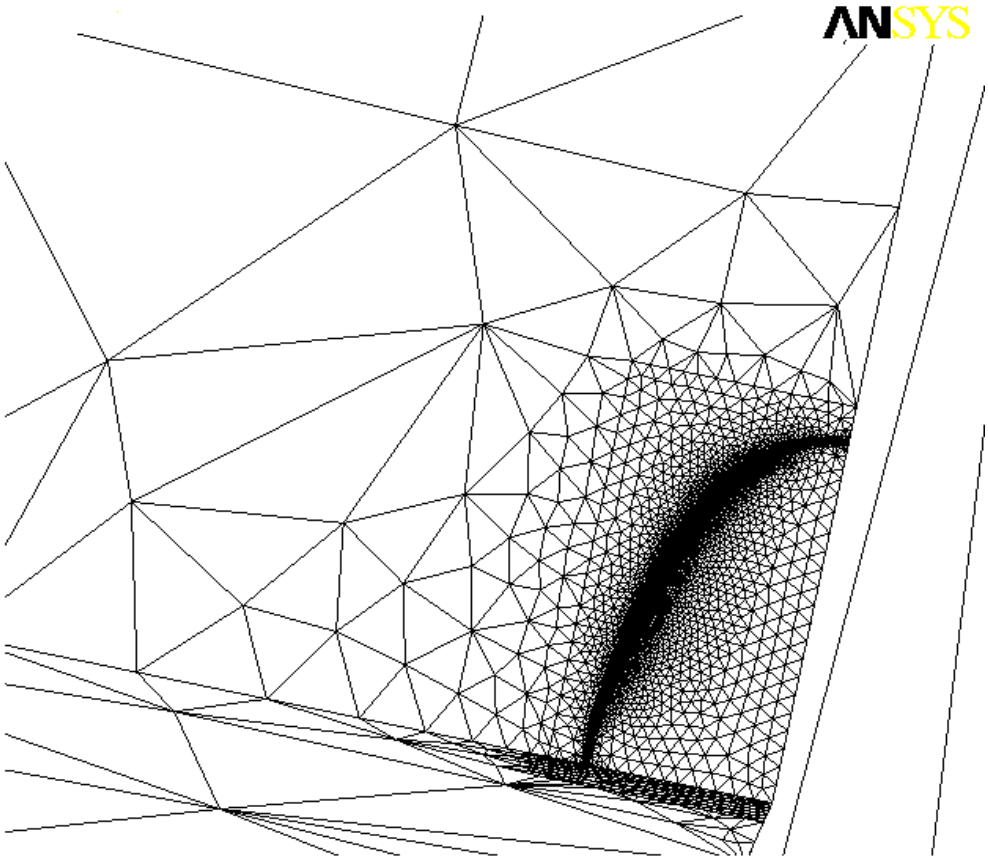

Figure 4.3 A closer view of the crack on pressure vessel

Table 4.1 shows the crack lengths obtained from Marshall distribution.

Table 4.1 Crack length

Pa from Marshall Distribution	a (cm)
0.72614885	0.039
0.06946752	0.044
0.00562507	0.134
0.00021033	0.252
0.00001118	0.357
0.00000096	0.445
0.00000011	0.522

The comparison between stress intensity factor and fracture toughness is performed and propagation of the crack (whether it is propagated or not) is observed.

From the results, it is seen that the crack has the most dangerous values for the biggest initial crack value. Then for five different a over c values the same analysis are performed and the stress intensity factor and fracture toughness values are compared. The a over c values are taken as 1/2, 1/3, 1/4 and 1/5, respectively. It is observed that for the smallest a over c value, which is 1/5, the crack propagates.

In the last part, crack is enlarged by multiplying a and c values with 2, 3 and 4, respectively. And the same analyses for rest of four a/c values are done. When two times of a and two times of c are taken, crack began to propagate in the third step in which a over c is taken as 1/3.

Then the crack is enlarged three times and four times, respectively and the same analyses are performed. It is seen that crack starts to propagate at earlier time steps as expected.

4.2 Results

In the first part, there are seven cases. These depend on the crack size according to Marshall distribution. The analysis goes from the smallest crack size to the biggest one.

4.2.1 Case 1

For Pa=0.72614885 from Marshall distribution, which means a = 0.039 cm, Figure 4.4 (a) shows the temperature distribution as a function of time. In Figure 4.4 (a) temperature distribution after analysis is given for two different points on crack. TEMPA is the temperature on point a and TEMPC is the temperature on point c of the elliptical crack. These temperature values on crack tip points have a distribution close to the temperature distribution in SBLOCA.

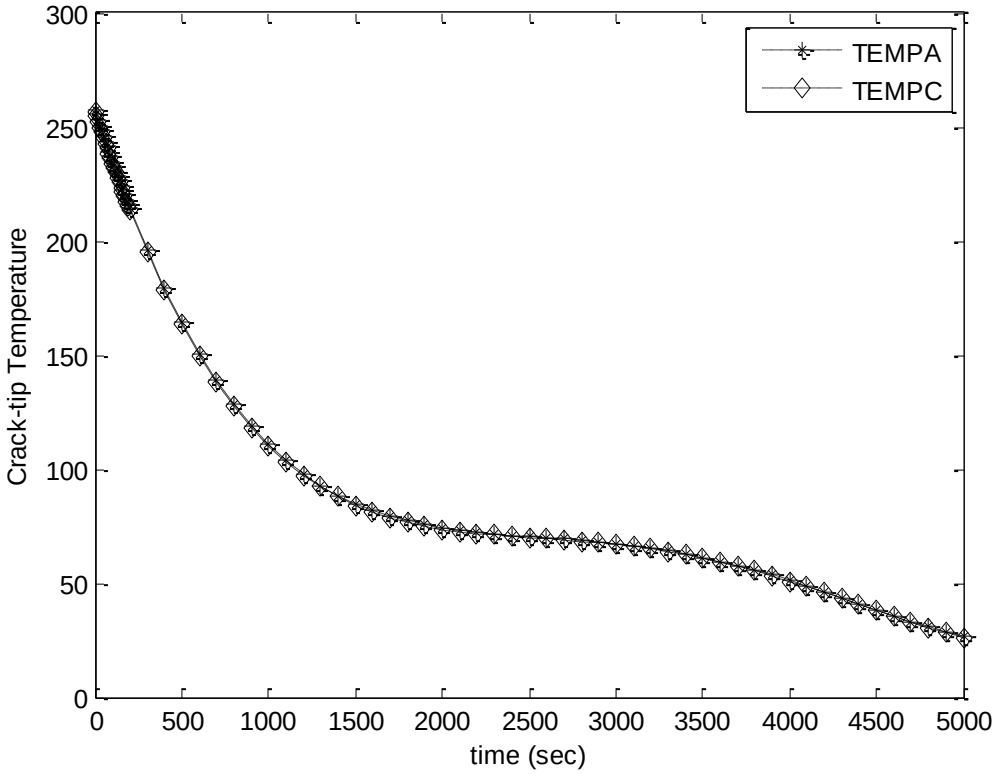

Figure 4.4 (a) Temperature distribution as a function of time

As explained above, the initial temperature is taken as 300 ^{0}C for the analysis done. Temperature distribution in case of SBLOCA is given in Figure 2.3 and after having thermal analysis in 2D axisymmetric geometry using values of

temperature in Figure 2.3, the temperature distribution in the reactor pressure vessel is obtained and temperature equation is derived using these temperature values and this equation is used in the code as input as a function of location and time.

In the analysis, to check the accuracy of the code, another point b is defined. b is taken between a and c crack tip points. And in Figure 4.4 (b) stress intensity and fracture toughness values are given in 5000 sec. KTA is the stress intensity on point a, KTB is the stress intensity on point b and KTC is the stress intensity on point c. KICA is the fracture toughness value for crack initiation on point a and KICC is the fracture toughness for crack initiation on point c.

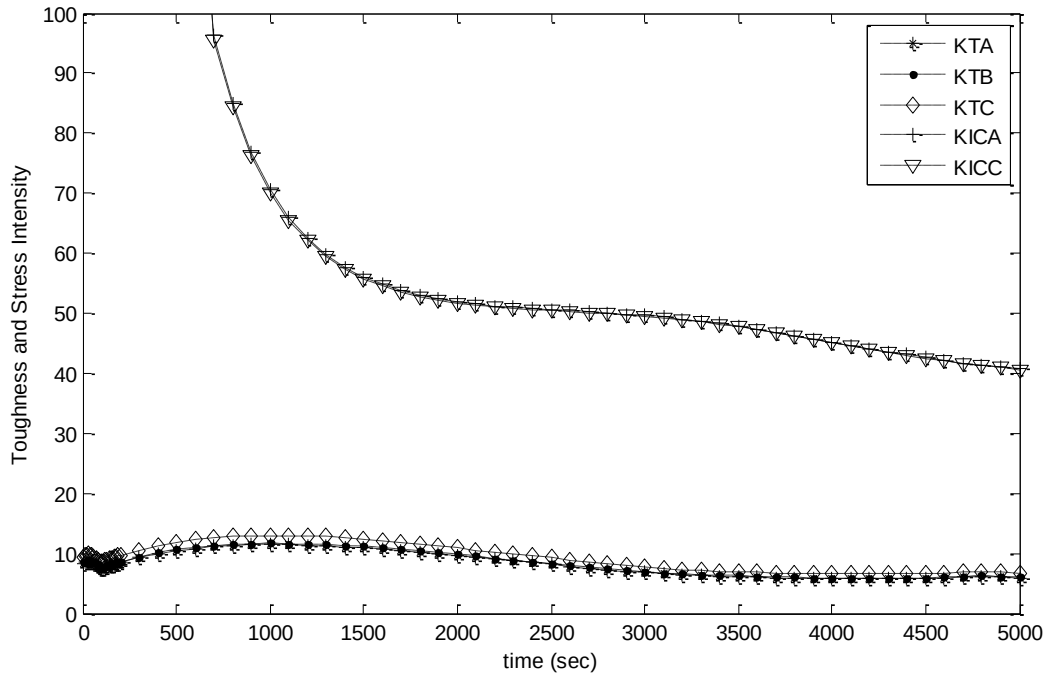

Figure 4.4 (b) Variation of stress intensity and fracture toughness values as a function of time

4.2.2 Case 2

For Pa=0.06946752 from Marshall Distribution, which means a = 0.044cm, temperature distribution and variation of stress intensity and fracture toughness values as a function of time are presented in Figures 4.5 (a) and 4.5 (b).

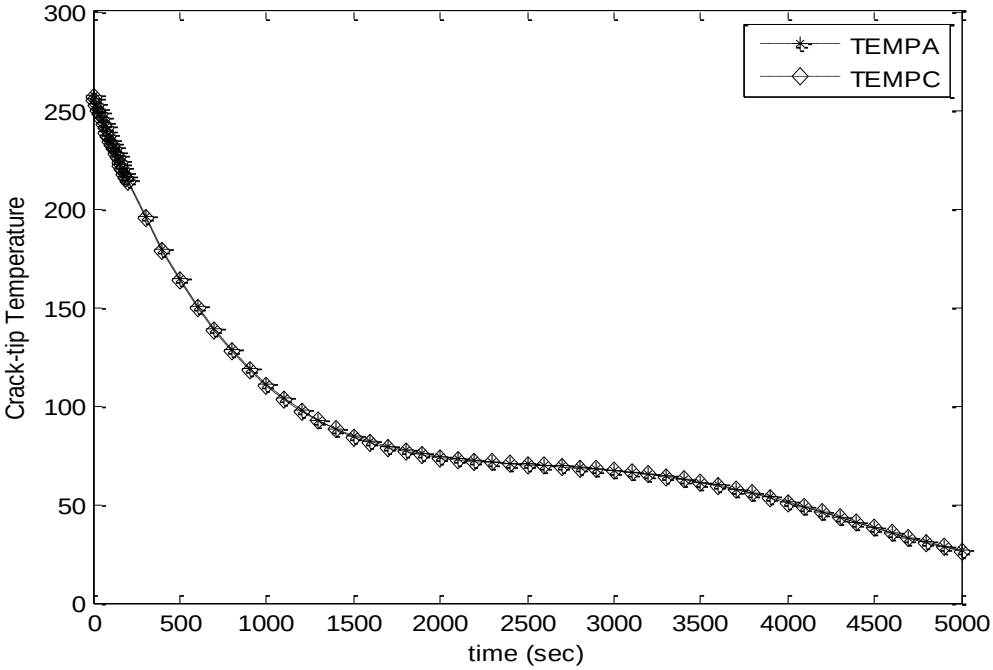

Figure 4.5 (a) Temperature distribution as a function of time

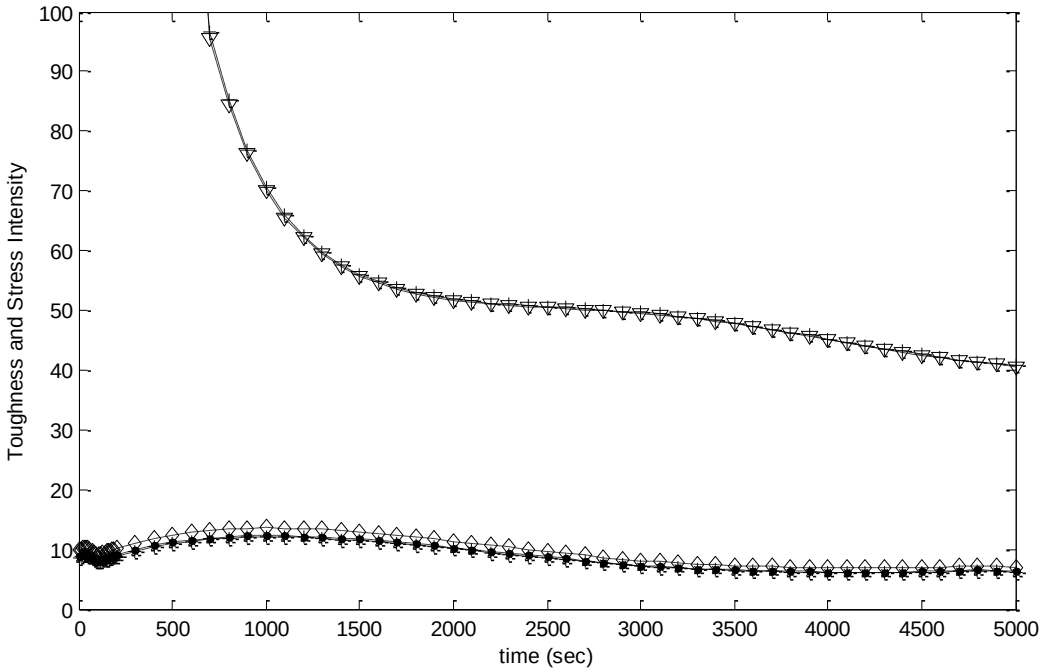

Figure 4.5 (b) Variation of stress intensity and fracture toughness values as a function of time

4.2.3 Case 3

Temperature distribution and variation of stress intensity and fracture toughness values as a function of time for Pa=0.00562507 from Marshall Distribution, which means a = 0.134cm, are presented in Figures 4.6 (a) and 4.6 (b).

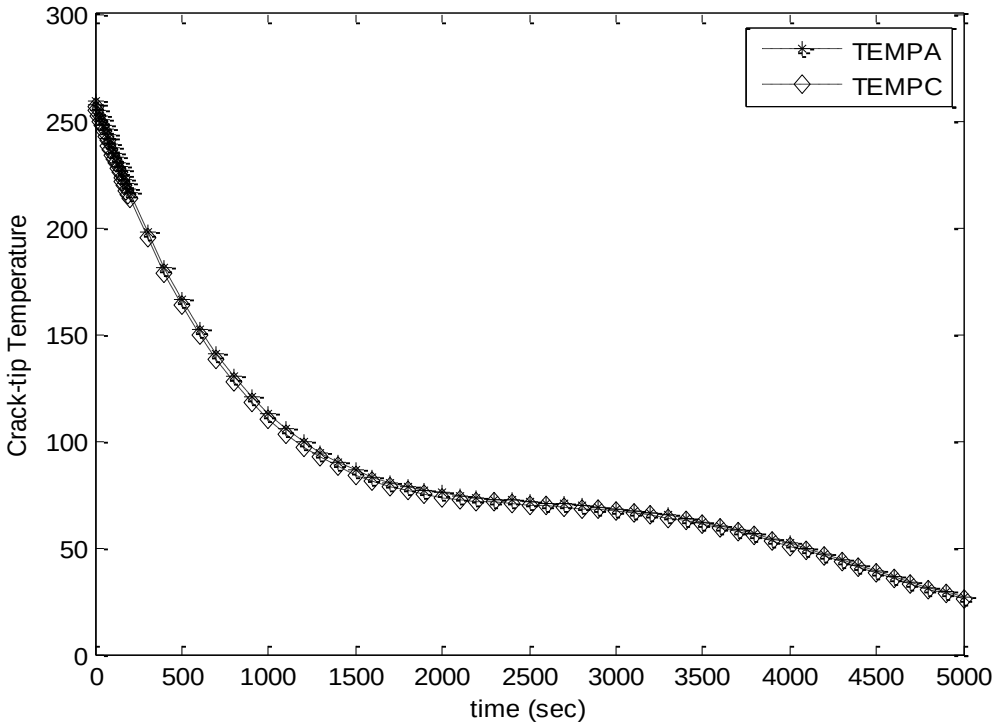

Figure 4.6 (a) Temperature distribution as a function of time

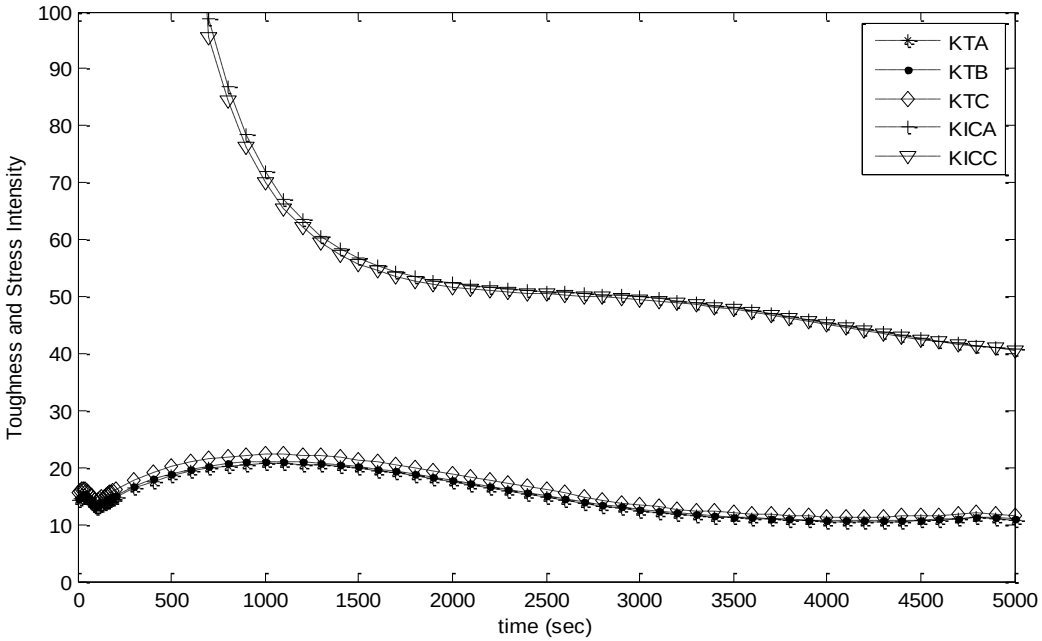

Figure 4.6 (b) Variation of stress intensity and fracture toughness values as a function of time

4.2.4 Case 4

For Pa=0.00021033 from Marshall Distribution, which means a = 0.252 cm, Figures 4.7 (a) and 4.7 (b) present temperature distribution and variation of stress intensity and fracture toughness values as a function of time.

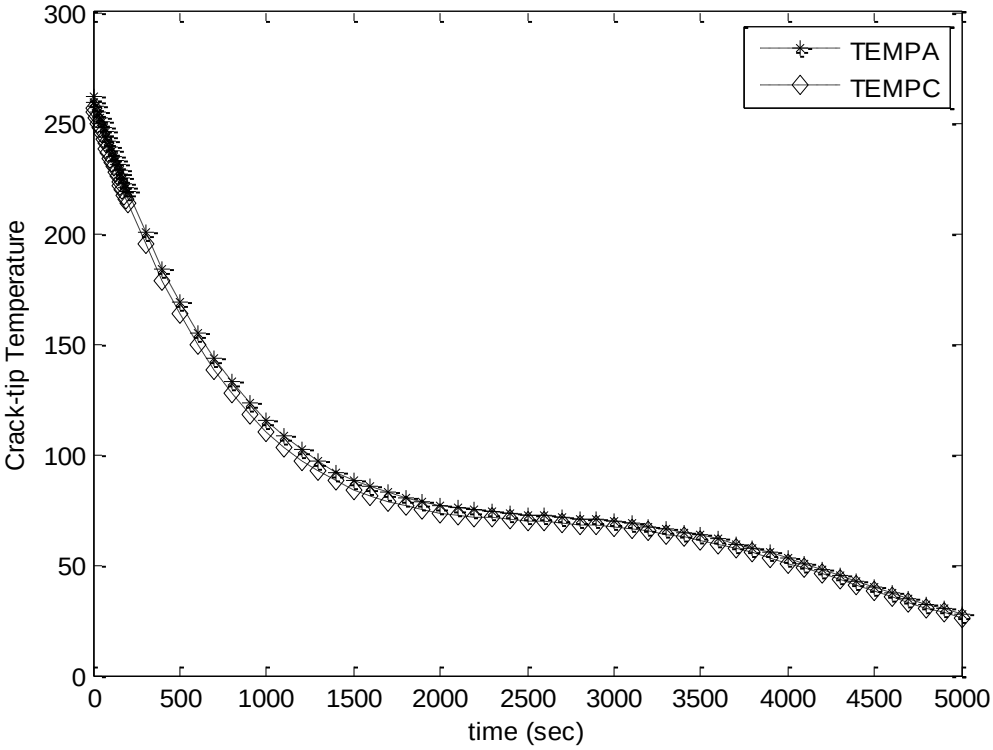

Figure 4.7 (a) Temperature distribution as a function of time

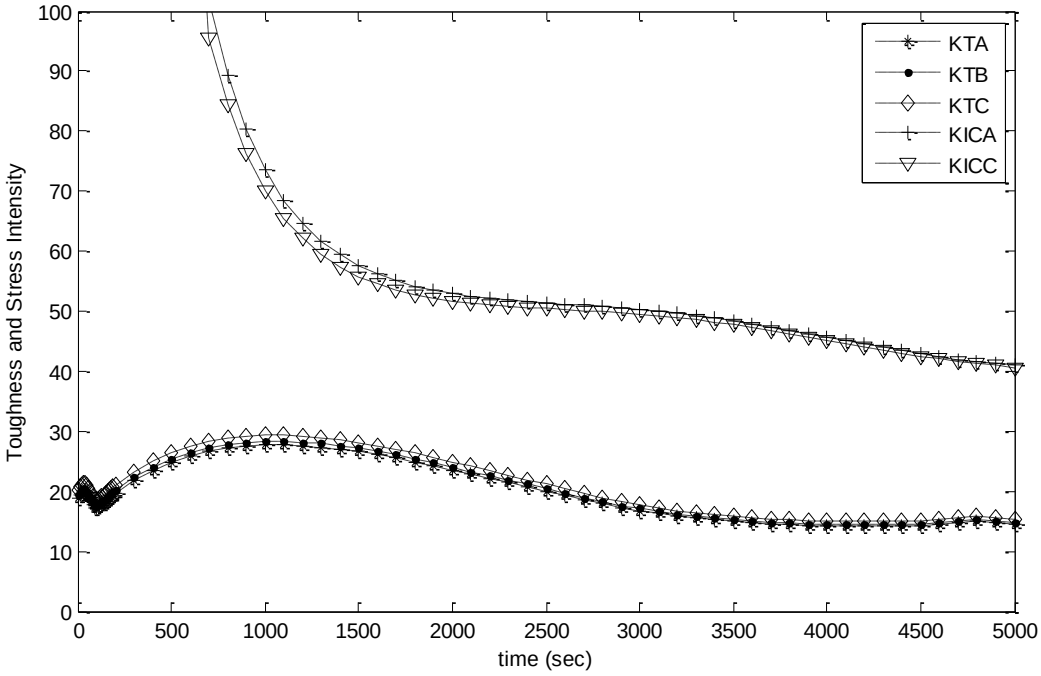

Figure 4.7 (b) Variation of stress intensity and fracture toughness values as a function of time

4.2.5 Case 5

In Figures 4.8 (a) and 4.8 (b), for Pa=0.00001118 from Marshall Distribution, which means a = 0.357 cm, temperature distribution and variation of stress intensity and fracture toughness values as a function of time are presented.

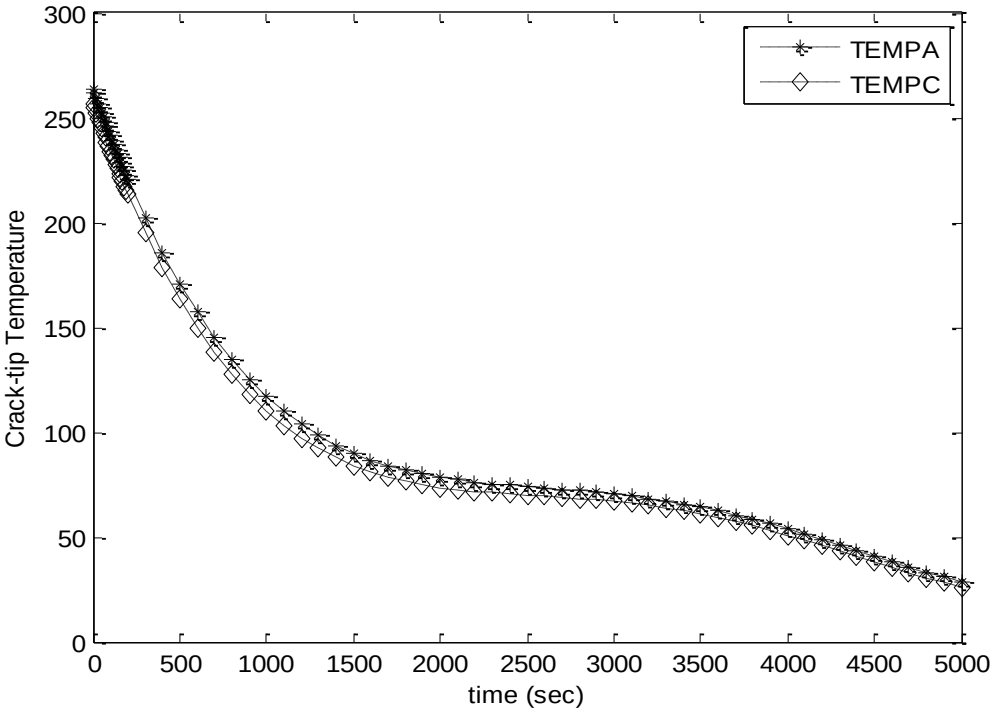

Figure 4.8 (a) Temperature distribution as a function of time

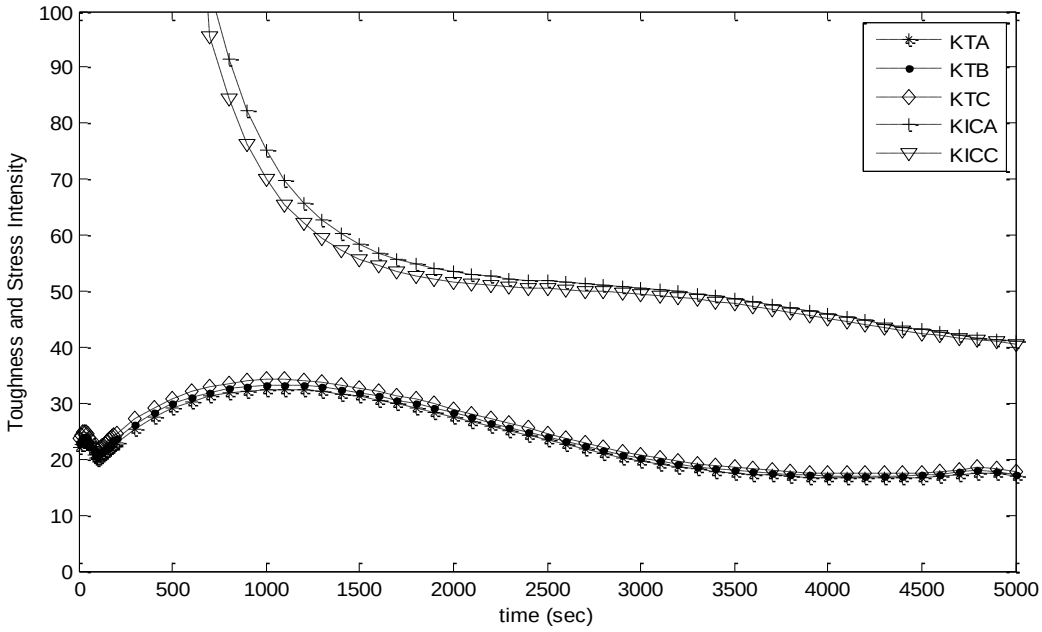

Figure 4.8 (b) Variation of stress intensity and fracture toughness values as a function of time

4.2.6 Case 6

For Pa=0.00000096 from Marshall Distribution, which means a = 0.445 cm, Figures 4.9 (a) and 4.9 (b) present temperature distribution and variation of stress intensity and fracture toughness values as a function of time.

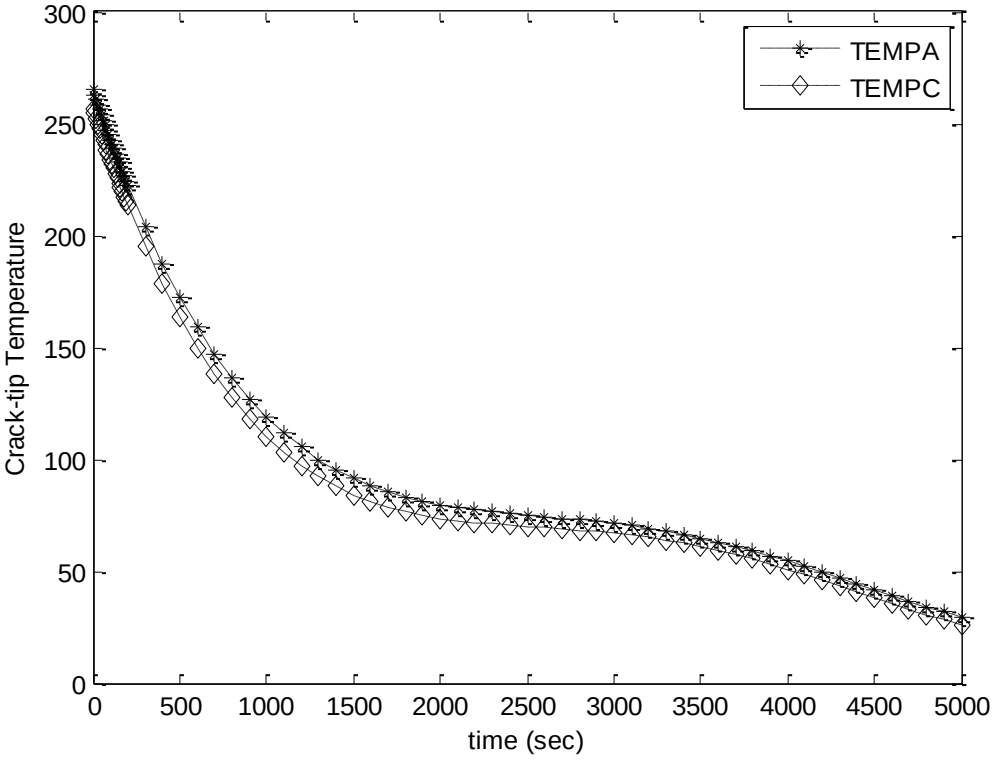

Figure 4.9 (a) Temperature distribution as a function of time

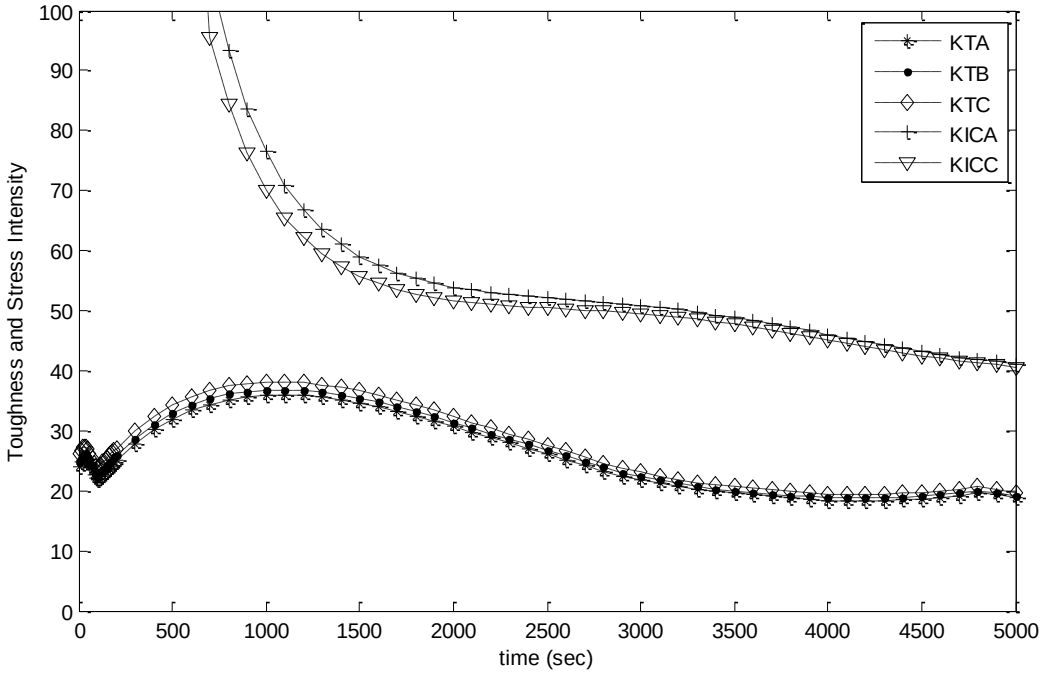

Figure 4.9 (b) Variation of stress intensity and fracture toughness values as a function of time

4.2.7 Case 7

For Pa=0.00000011 from Marshall Distribution, which means a = 0.522 cm, temperature distribution and variation of stress intensity and fracture toughness values as a function of time are presented in Figures 4.10 (a) and 4.10 (b), respectively.

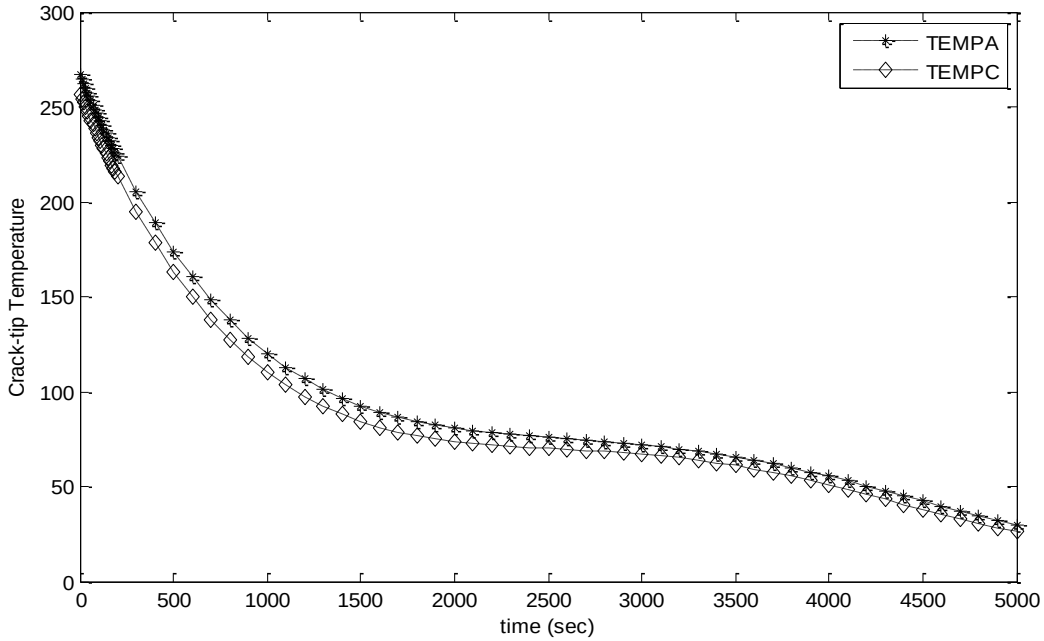

Figure 4.10 (a) Temperature distribution as a function of time

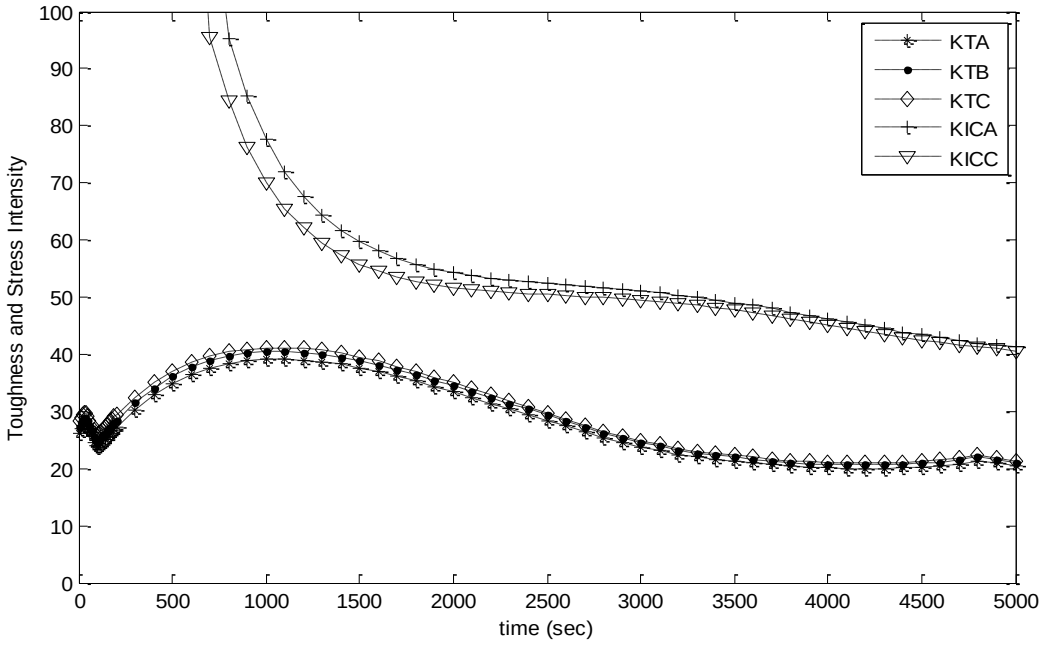

Figure 4.10 (b) Variation of stress intensity and fracture toughness values as a function of time

In all cases stress intensity and fracture toughness values on crack tips are compared. It is observed that these values are closer when crack size gets bigger. And in all cases KTB values for all crack sizes are between KTA and KTC values as expected.

According to these analysis and the above graphs, it is seen that when the crack size gets bigger, it becomes more dangerous. So that it may cause failure of the reactor pressure vessel. The difference between fracture toughness values and stress intensity values are getting smaller which also shows that the crack becomes closer to the propagation.

4.2.8 The Crack Analysis for the Biggest Initial Crack Size

For the biggest crack size new analysis are done for four more a over c values which are 1/2, 1/3, 1/4 and 1/5, respectively.

For a over c = ½

For the biggest crack length (a), a over c is taken as ½

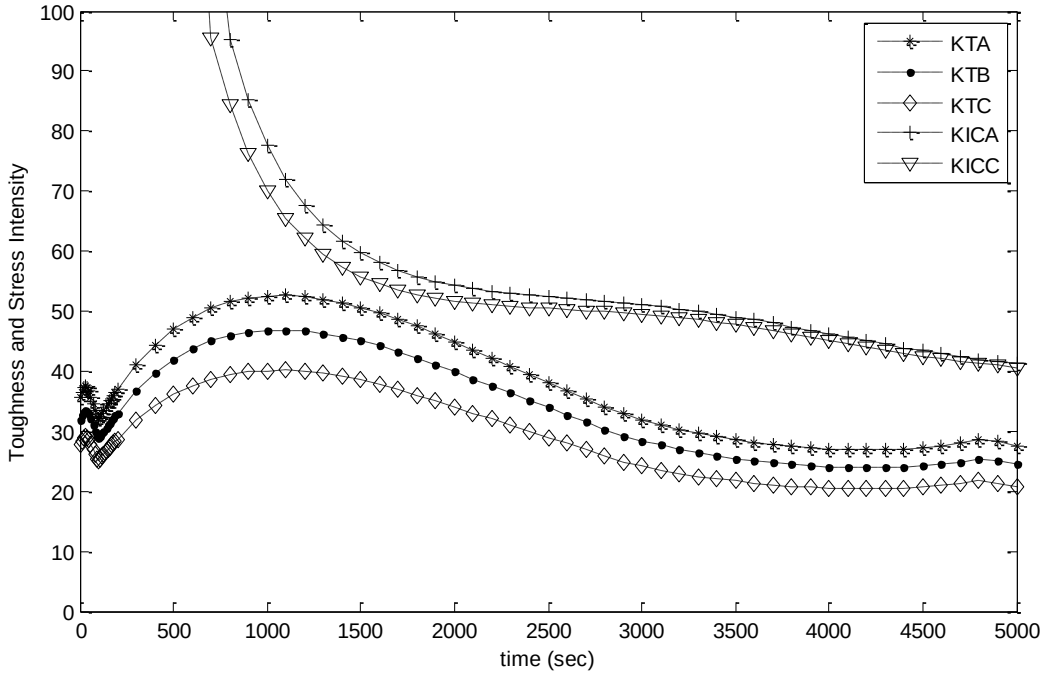

Figure 4.11 Variation of stress intensity and fracture toughness values as a function of time

When a over c is 1/3

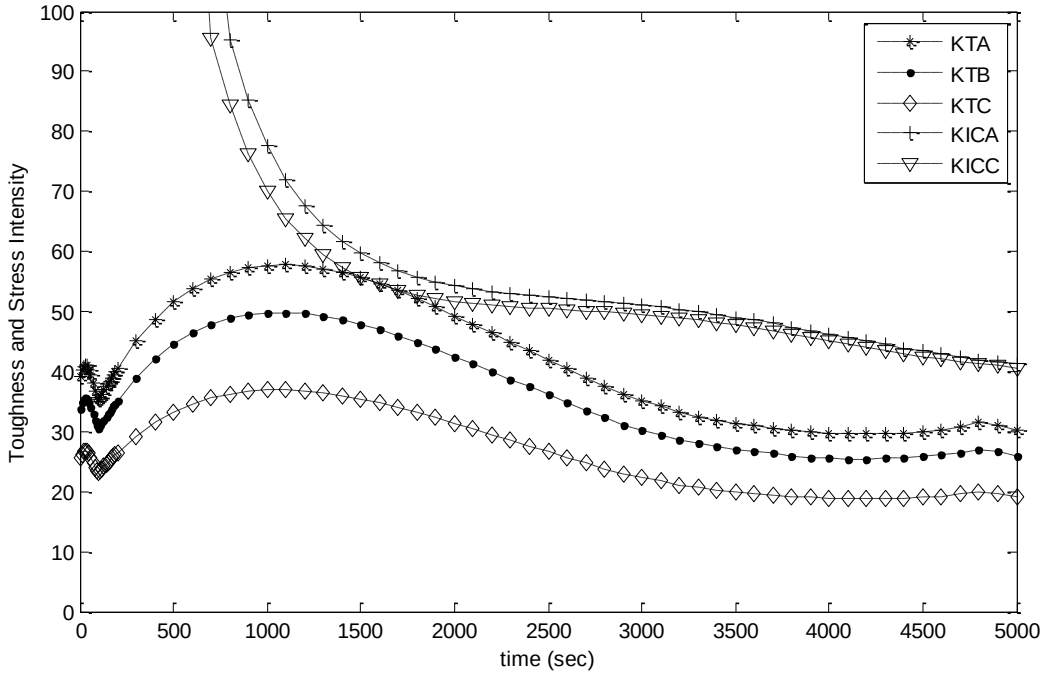

Figure 4.12 Variation of stress intensity and fracture toughness values as a function of time

For a over c = ¼

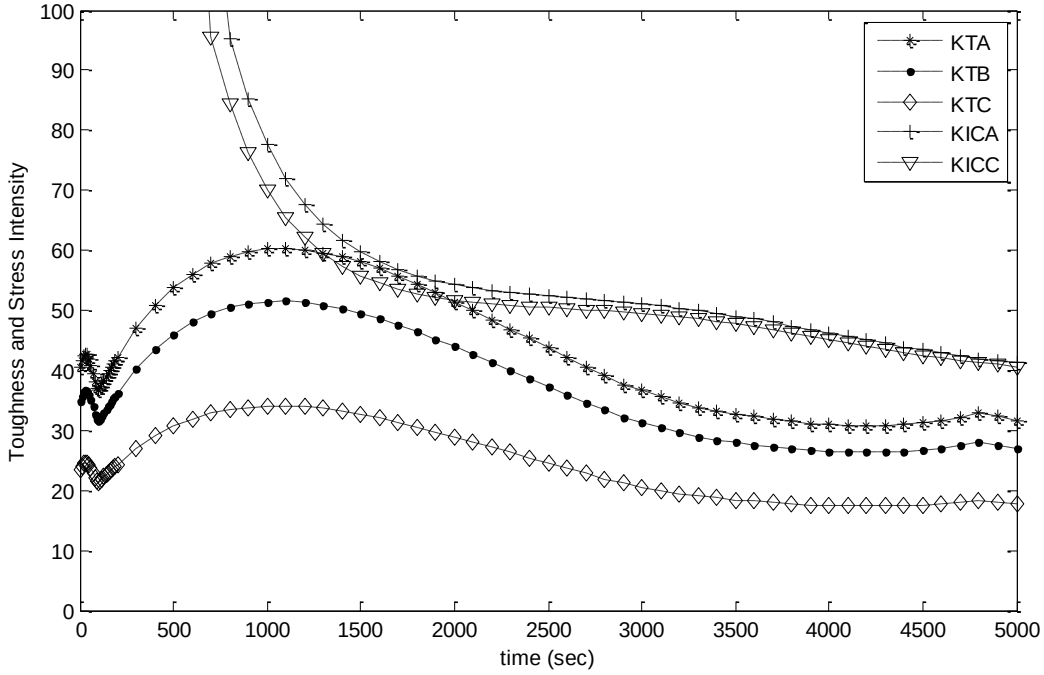

Figure 4.13 Variation of stress intensity and fracture toughness values as a function of time

For the analysis in cases of a/c is 1/2, 1/3 and 1/4, stress intensity and fracture toughness for crack initiation values are compared. Fracture toughness values for crack initiation are still higher than stress intensity values in ½ case. When a/c is taken as 1/3 and 1/4, stress intensity values begin to get higher from fracture toughness values for crack initiation which means crack may propagate.

Stress intensity and fracture toughness values come closer but do not intersect each other. But in this analysis some of the parameters, which are copper-nickel content, chemistry factor, initial crack size etc…,are taken as constant values. In real life, these values vary depending on pressure vessel designs, which may change the intersection of lines.

For the last step a over c is taken as 1/5

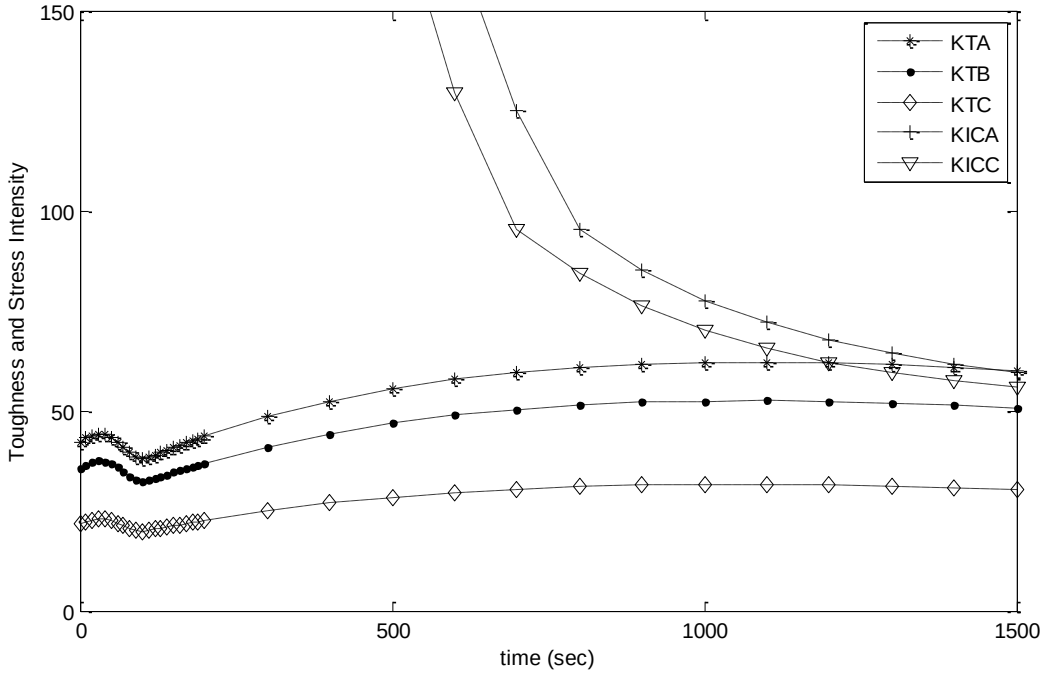

Figure 4.14 Variation of stress intensity and fracture toughness values as a function of time

For the first 1500 seconds the results are similar to the other ones. But when it comes to 1500th second, crack begins to propagate. And the comparison of fracture toughness for crack arrest and stress intensity shows if the crack arrests or not.

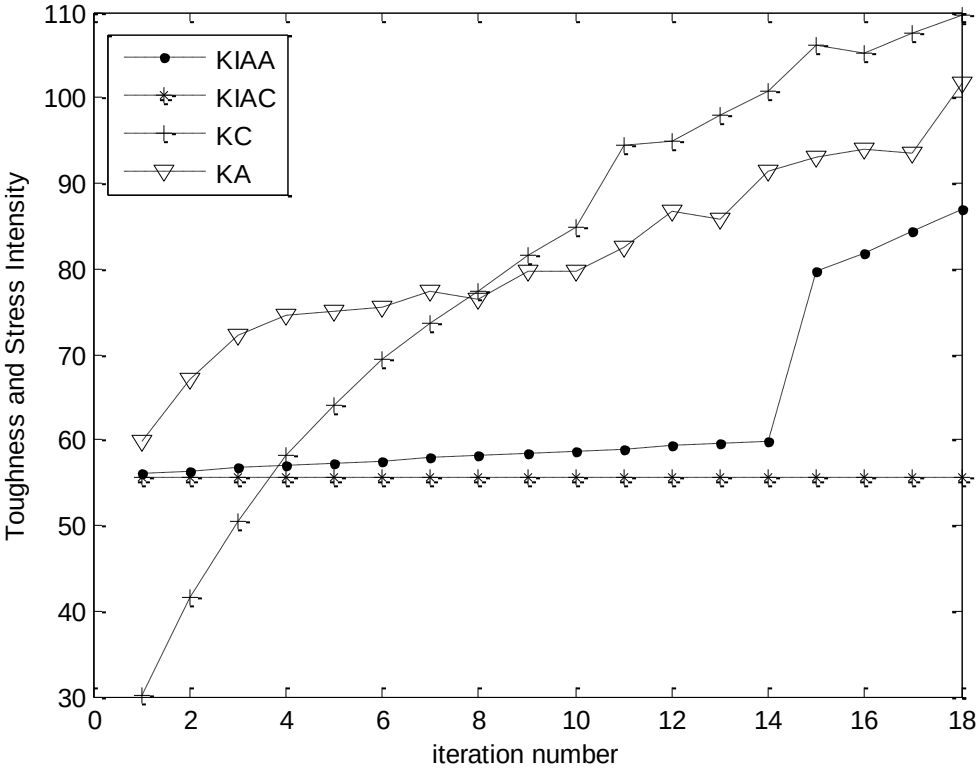

Figure 4.14 (a) Stress intensity and fracture toughness values as a function of iteration number

And the a/c values vs iteration number graph is as below:

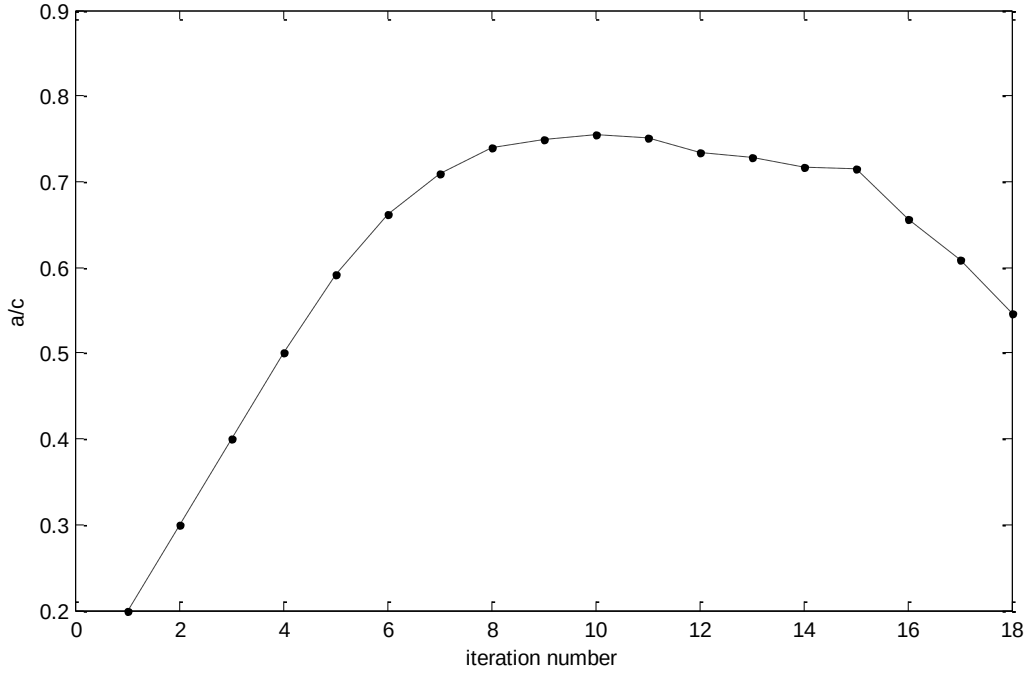

Figure 4.14 (b) Variation of a/c ratio as a function of iteration number

When the crack propagates, the crack front nodes are shifted by a/10 and depending on K_I^2 and K_{IA}^2 for a and c, respectively. Iteration number is the increment steps after the crack propagates.

When the crack size is bigger, it is seen that crack propagation probability is higher. According to this observation, for the new analysis, crack is extended two, three and four times, respectively and for all these three crack sizes, four different a/c ratios are analyzed.

a = 2a, c = 2c and a/c = 1

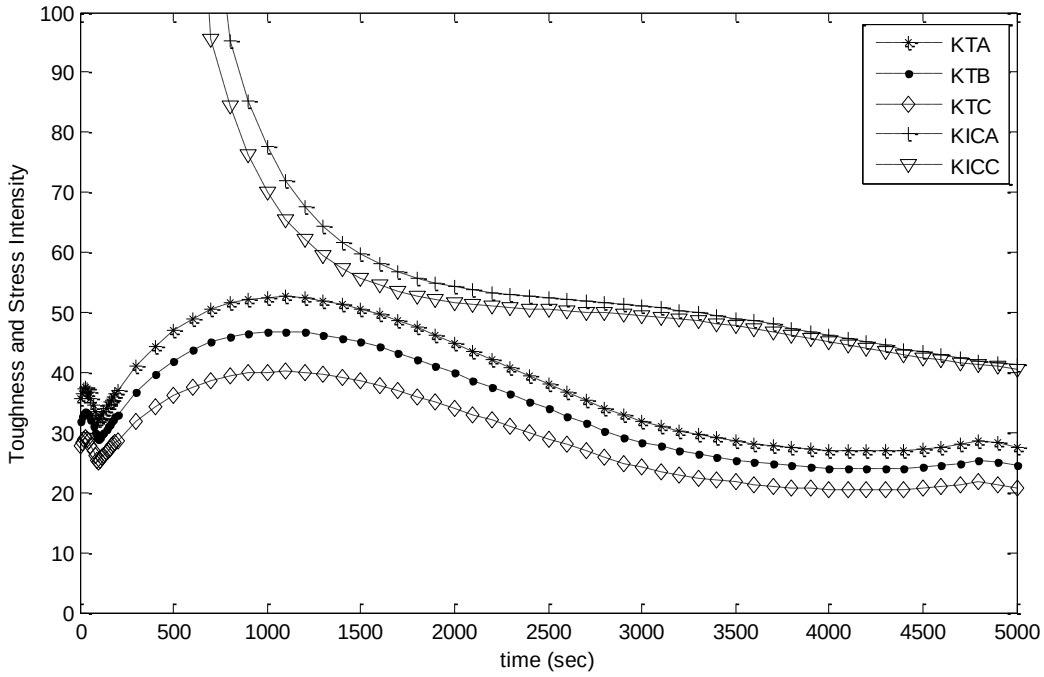

Figure 4.15 Variation of stress intensity and fracture toughness values as a function of time

a = 2a, c = 2c and a/c = ½

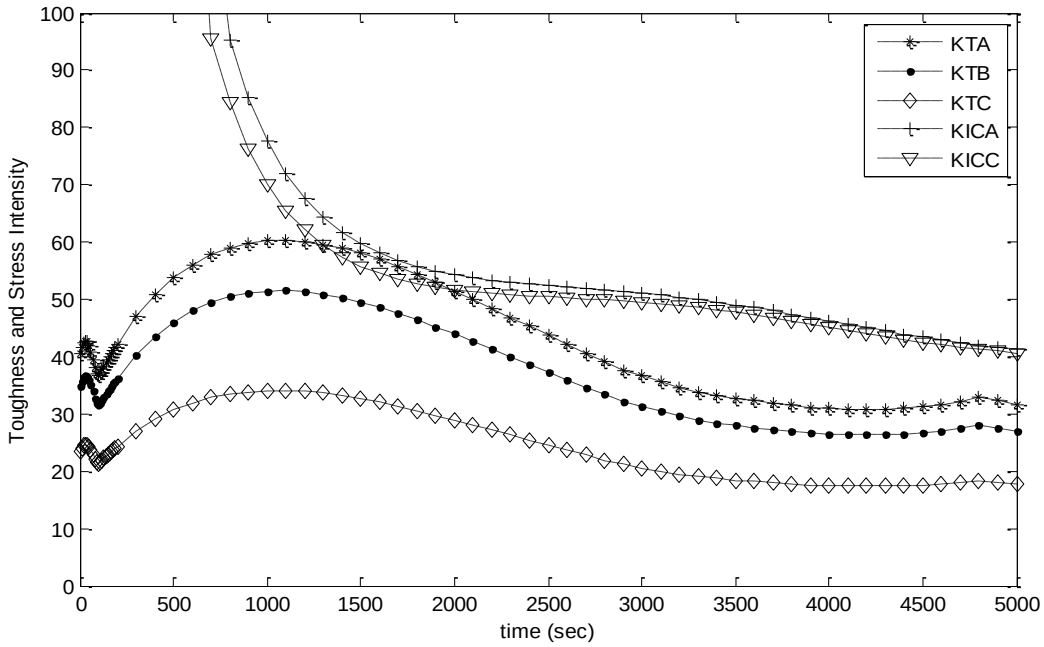

Figure 4.16 Variation of stress intensity and fracture toughness values as a function of time

a = 2a, c = 2c and a/c = 1/3

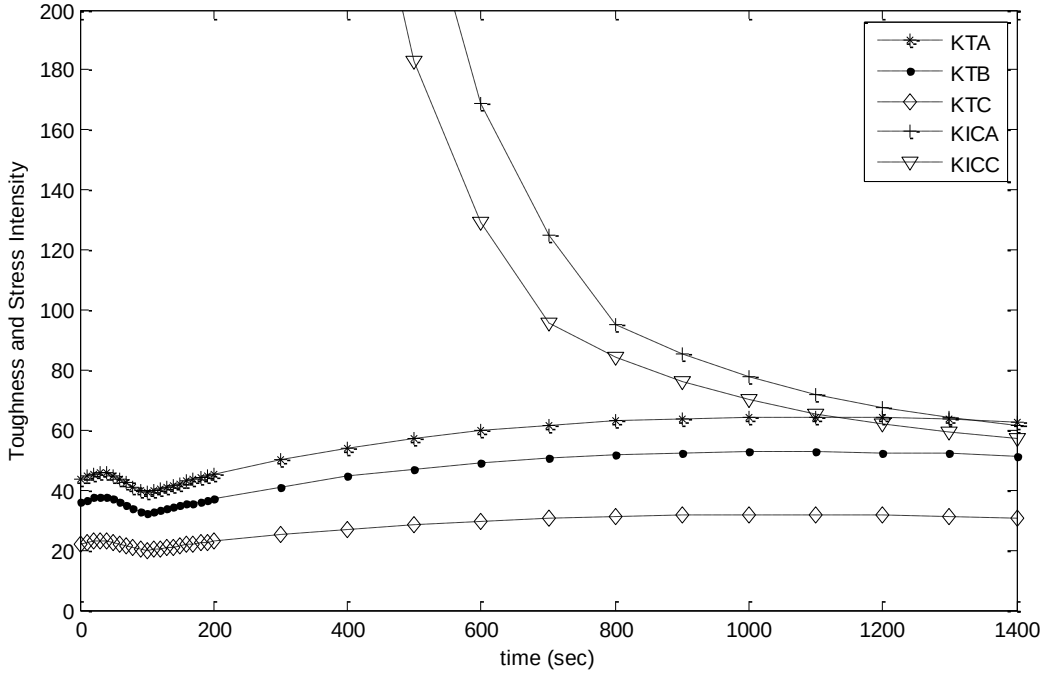

Figure 4.17 Variation of stress intensity and fracture toughness values as a function of time

For the first 1400 seconds the results are similar to the results of a/c=1/2. But when it comes to 1400th second, fracture toughness values for crack initiation becomes smaller than stress intensity values and crack propagates. To observe the propagation, fracture toughness values for crack arrest are examined.

In the 1400th second, fracture toughness for crack arrest values are given on the above graph. It is observed that crack can not be arrested which means it propagates.

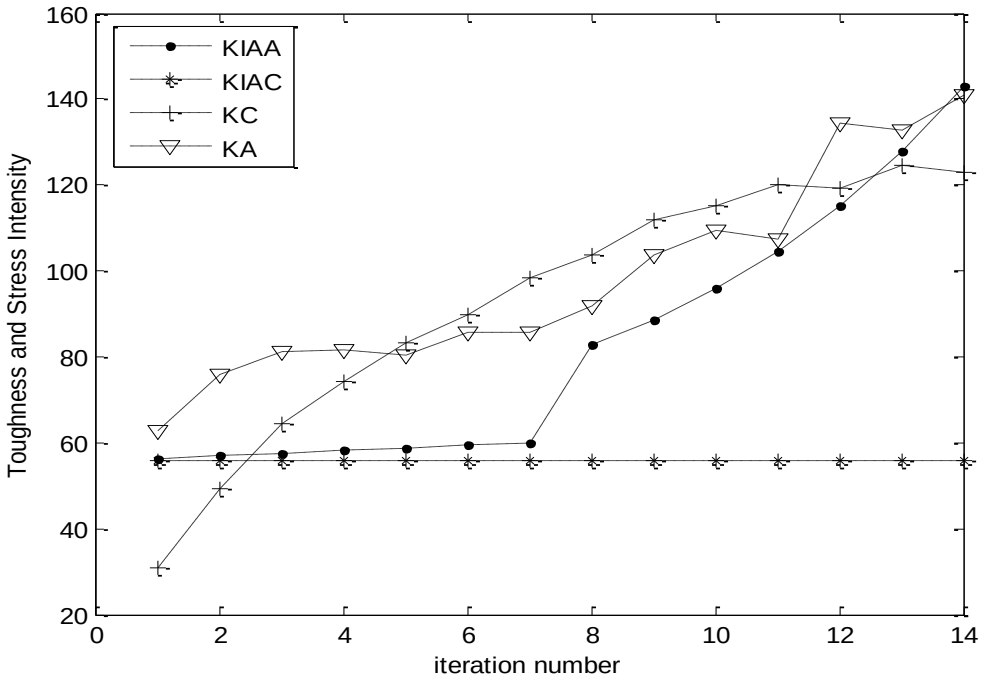

Figure 4.17 (a) Stress intensity and fracture toughness values as a function of iteration number

And the a/c values vs iteration number graph is as below. When a/c value goes to zero, the crack results in failure.

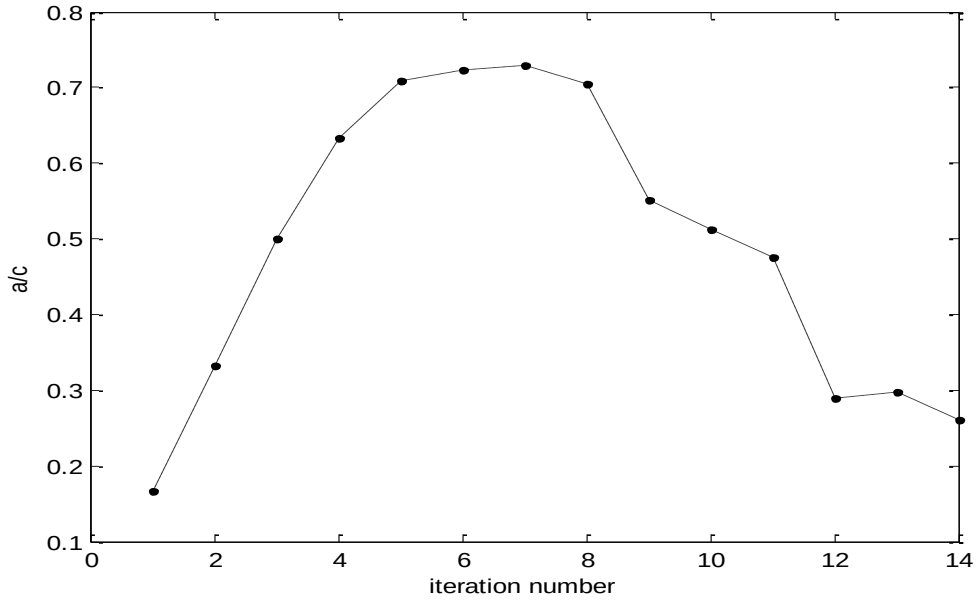

Figure 4.17 (b) Variation of a/c ratio as a function of iteration number

For smaller a/c values, almost the same results are expected.

a = 2a, c = 2c and a/c = ¼

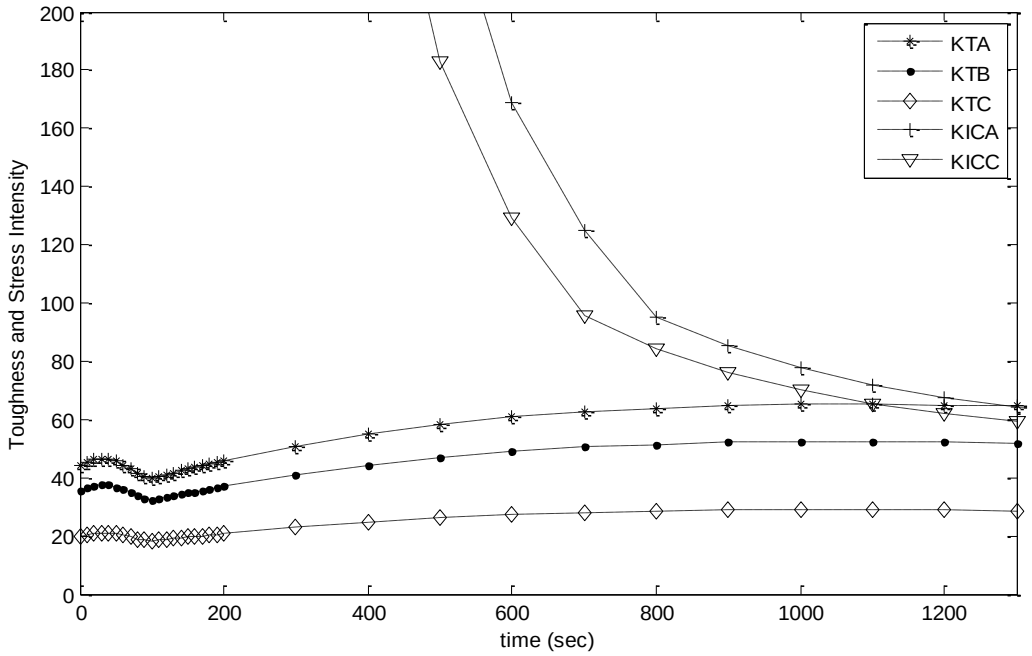

Figure 4.18 Variation of stress intensity and fracture toughness values as a function of time

After 1300th second, crack begins to propagate as can be seen below.

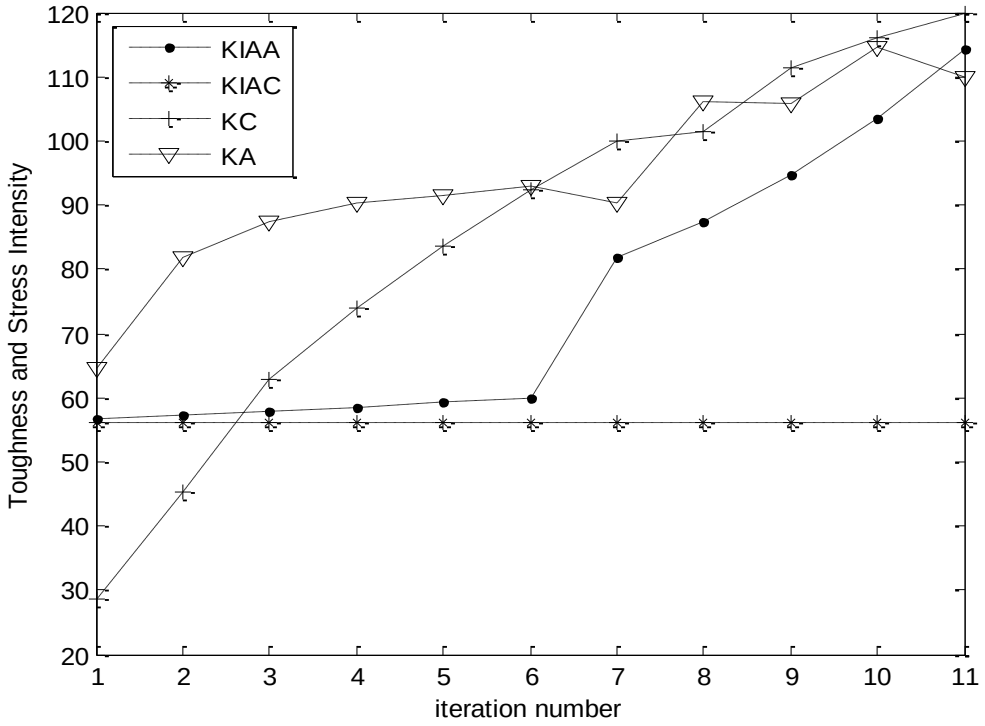

Figure 4.18 (a) Variation of stress intensity and fracture toughness values as a function of time

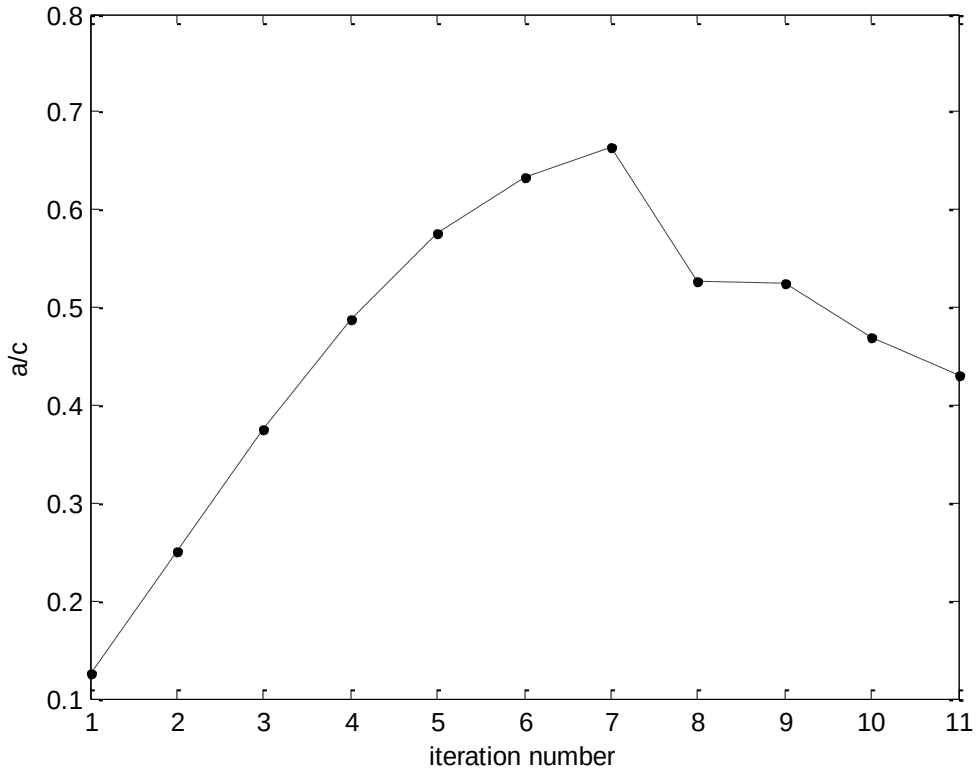

Figure 4.18 (b) Variation of a/c ratio as a function of iteration number

a = 2a, c = 2c and a/c = 1/5

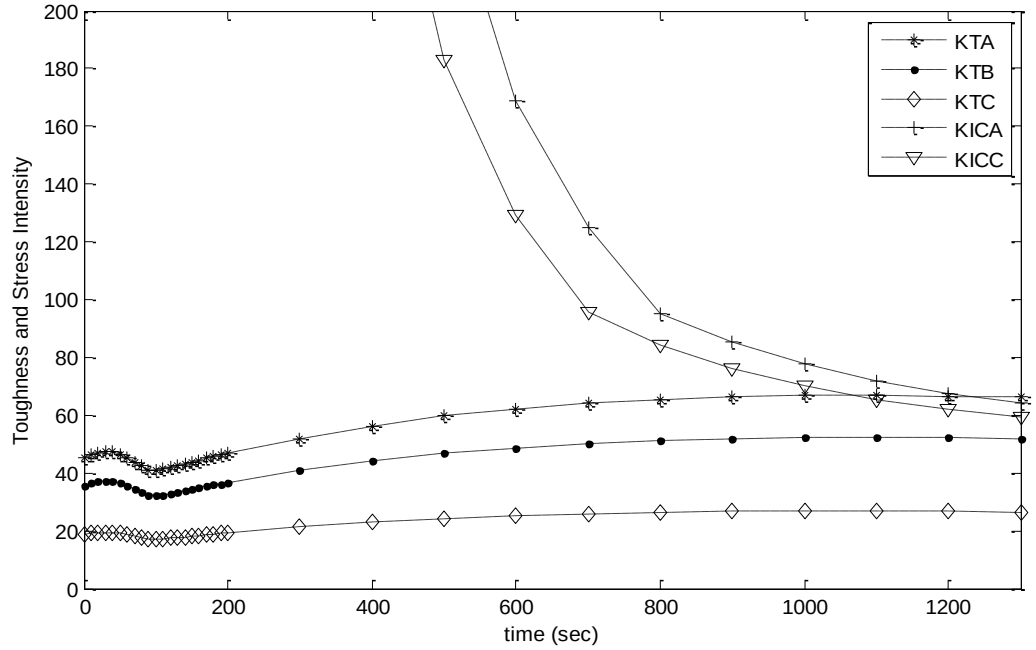

Figure 4.19 Variation of stress intensity and fracture toughness values as a function of time

For the first 1300 seconds the results are similar on the 1300th second, crack begins to propagate.

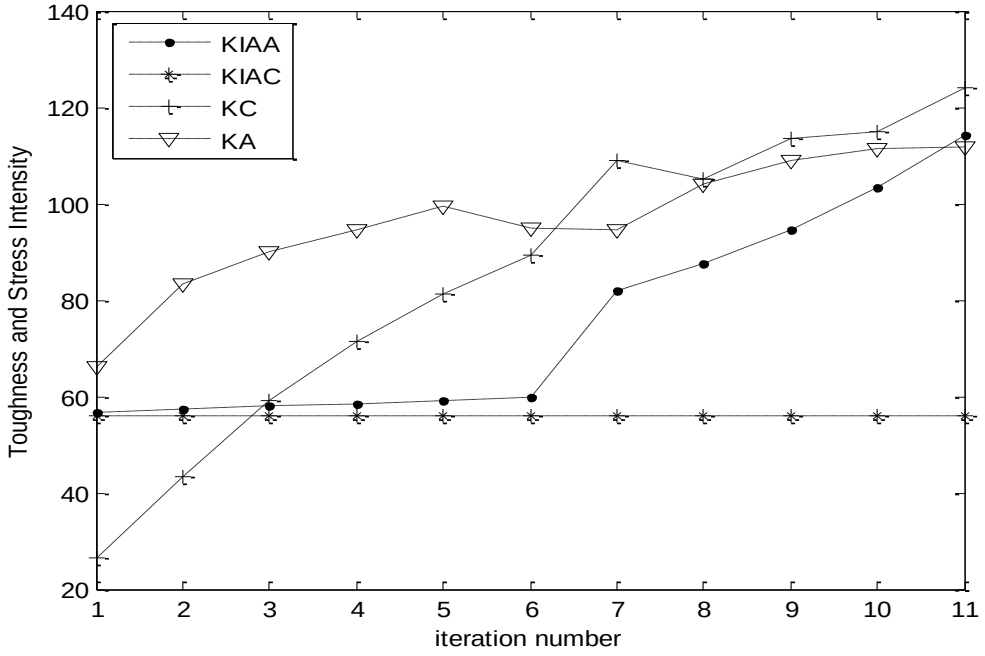

Figure 4.19 (a) Stress intensity and fracture toughness values as a function of iteration number

And the a/c values vs iteration number graph is as below:

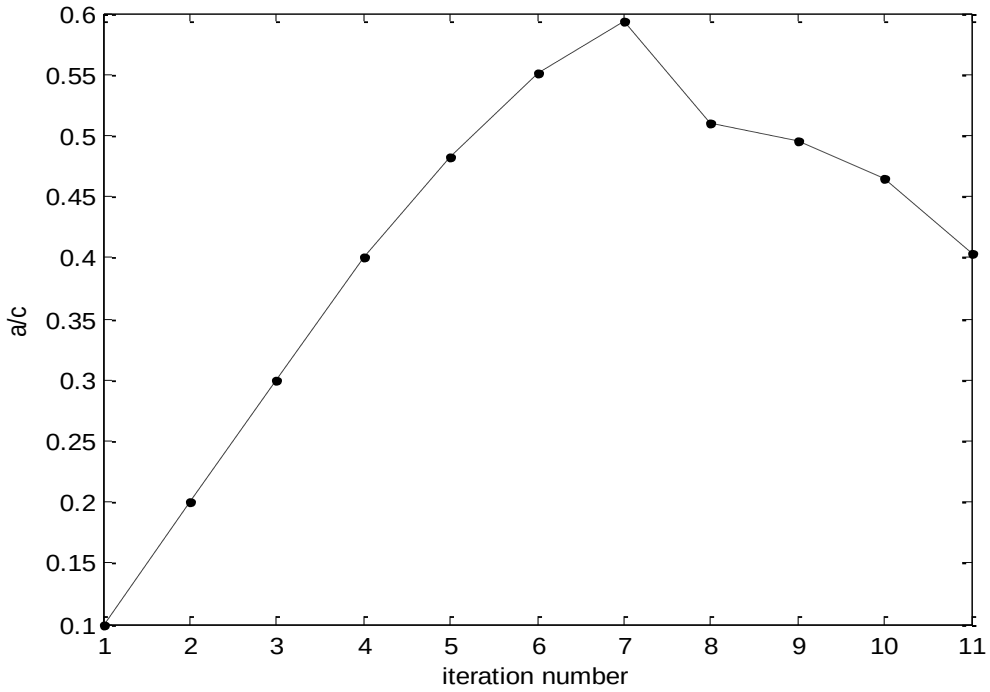

Figure 4.19 (b) Variation of a/c ratio as a function of iteration number

a = 3a, c = 3c and a/c = 1

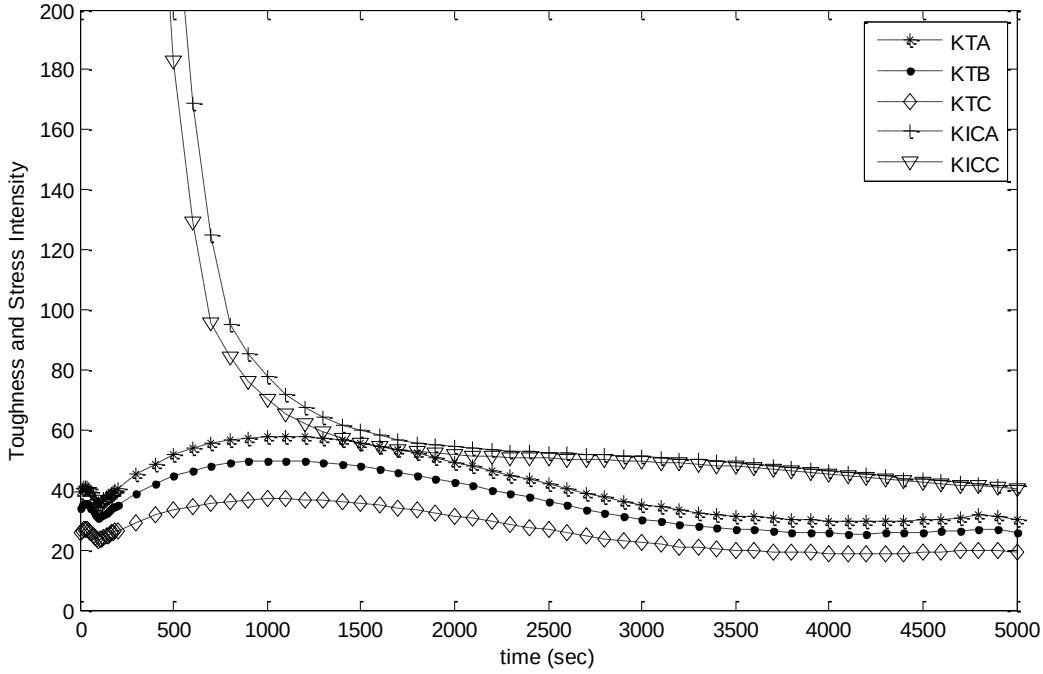

Figure 4.20 Variation of stress intensity and fracture toughness values as a function of time

a = 3a, c = 3c and a/c = ½

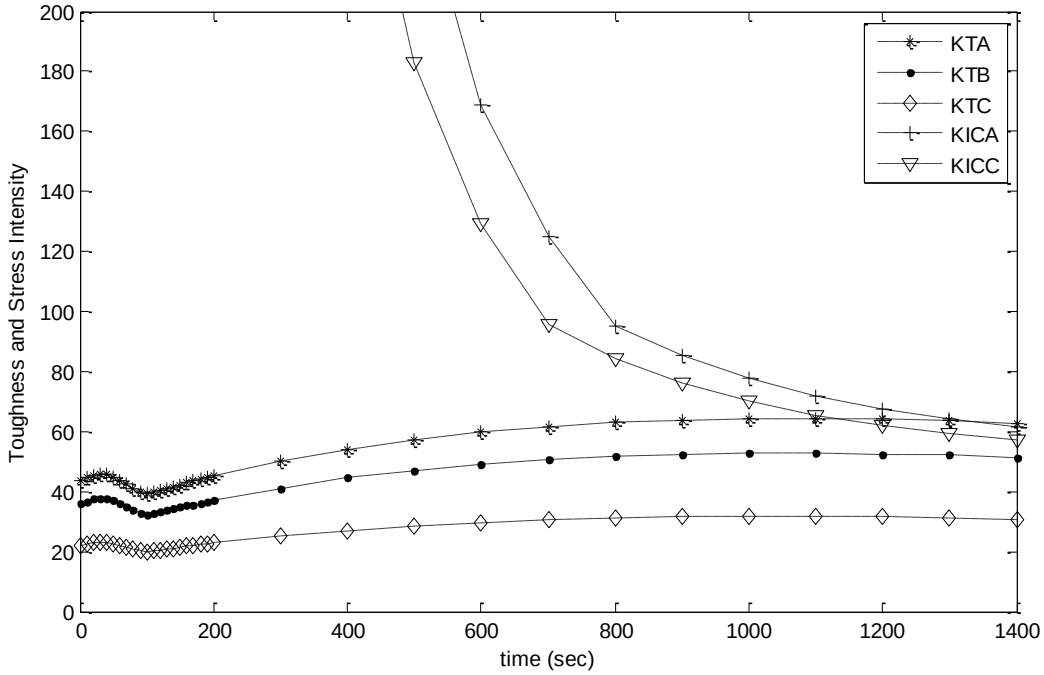

Figure 4.21 Variation of stress intensity and fracture toughness values as a function of time

For the first 1400 seconds stress intensity values are still lower than fracture toughness values. But on the 1400th second, crack begins to propagate. To see the propagation arrest values at points a and c are given on Figure 4.21 (a).

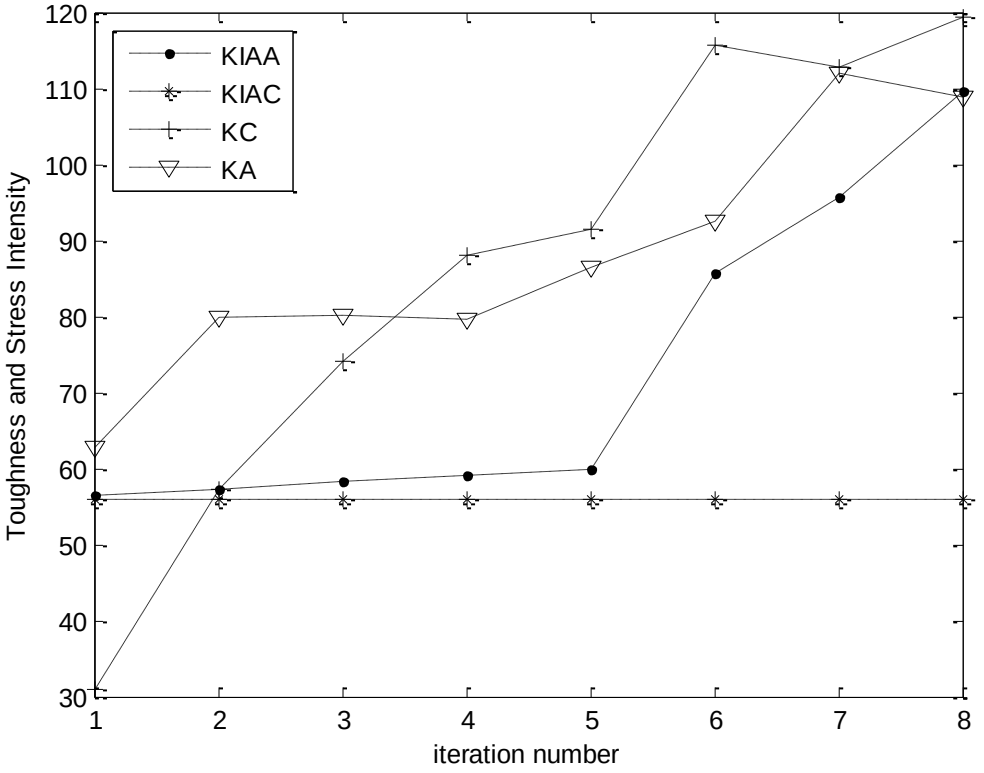

Figure 4.21 (a) Stress intensity and fracture toughness values as a function of iteration number

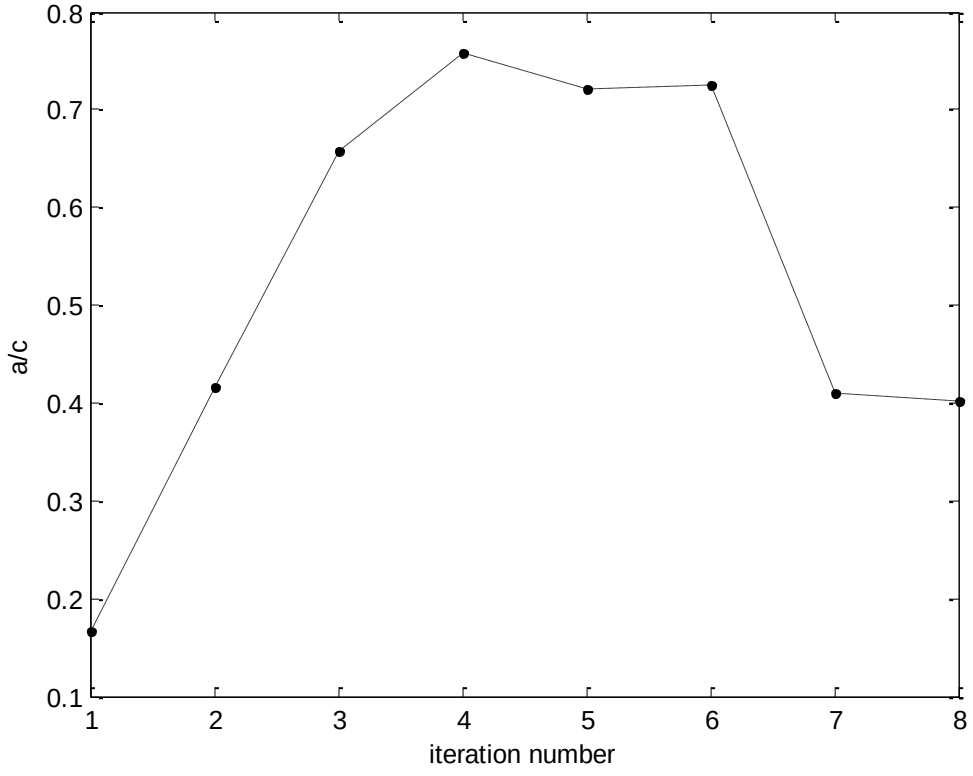

Figure 4.21 (b) Variation of a/c ratio as a function of iteration number

a = 3a, c = 3c and a/c = 1/3

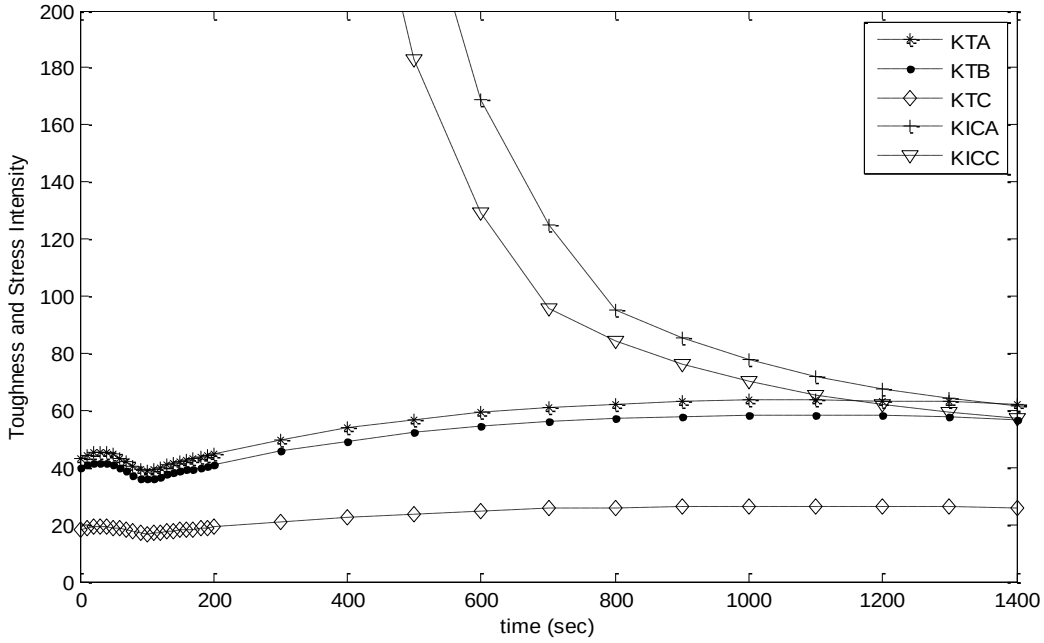

Figure 4.22 Variation of stress intensity and fracture toughness values as a function of time

For the first 1400 seconds the results are similar to the other ones. But when it comes to 1400th second, crack begins to propagate.

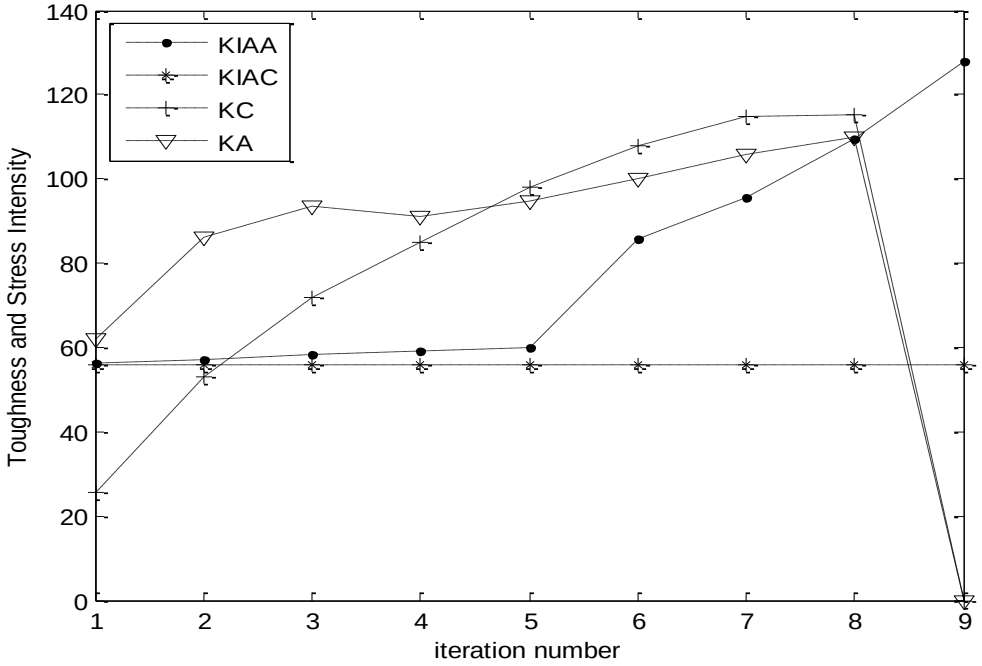

Figure 4.22 (a) Stress intensity and fracture toughness values as a function of iteration number

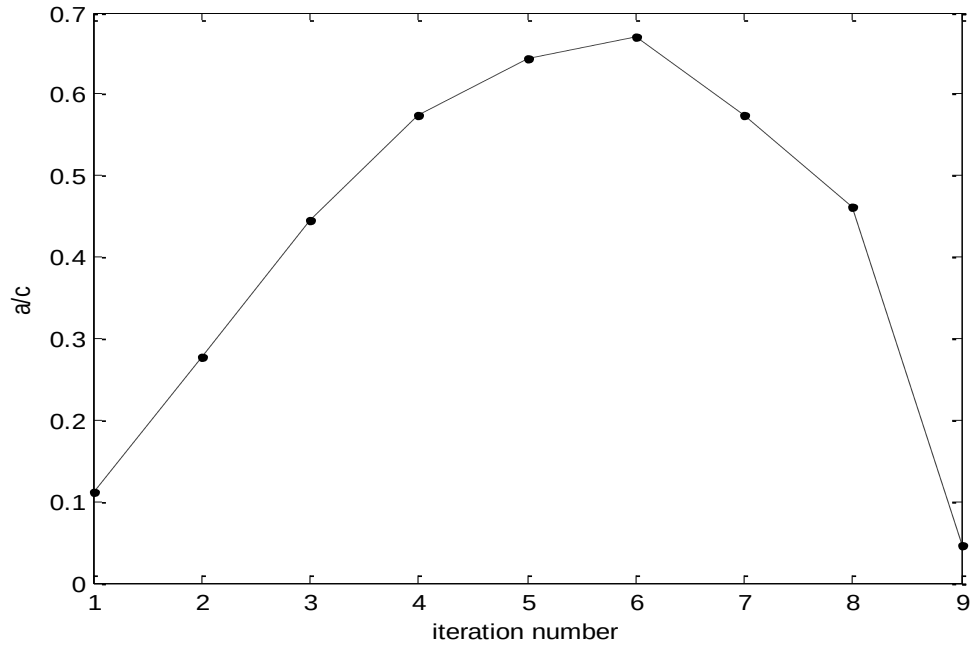

Figure 4.22 (b) Variation of a/c ratio as a function of iteration number

a = 3a, c = 3c and a/c = 1/4

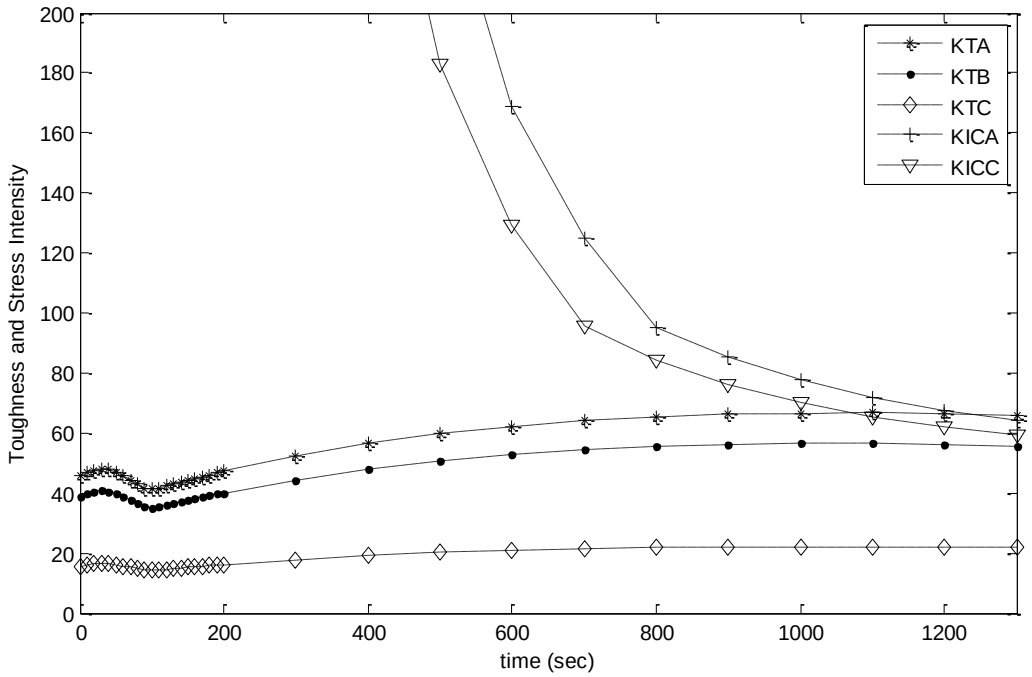

Figure 4.23 Variation of stress intensity and fracture toughness values as a function of time

For the first 1300 seconds the results are similar to the other ones. But when it comes to 1300th second, crack begins to propagate. To see the propagation arrest values at points a and c are given on below graph.

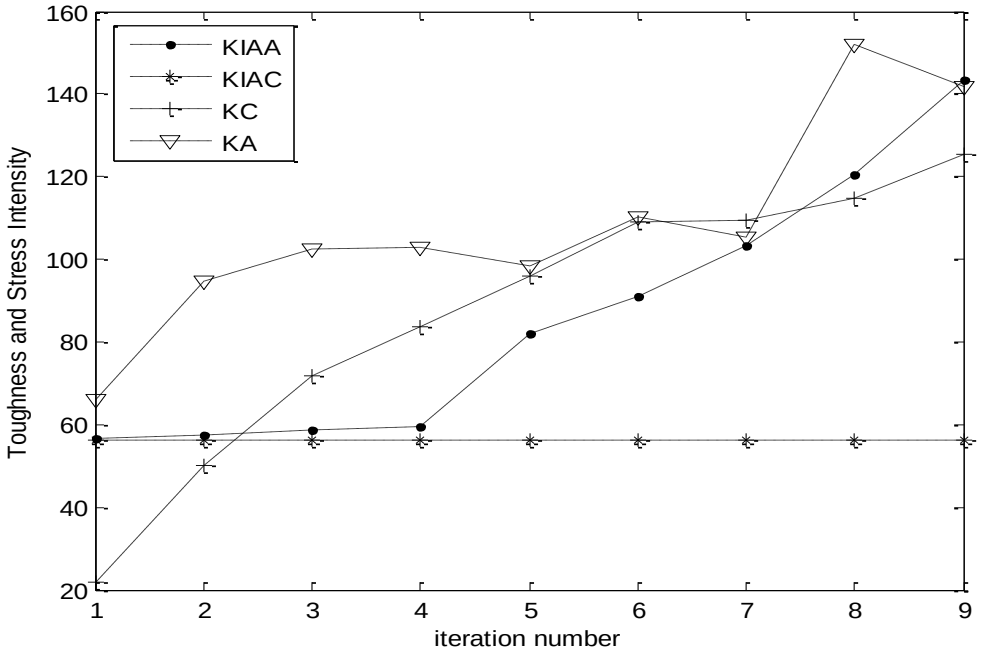

Figure 4.23 (a) Stress intensity and fracture toughness values as a function of iteration number

And the a/c values vs iteration number graph is as below:

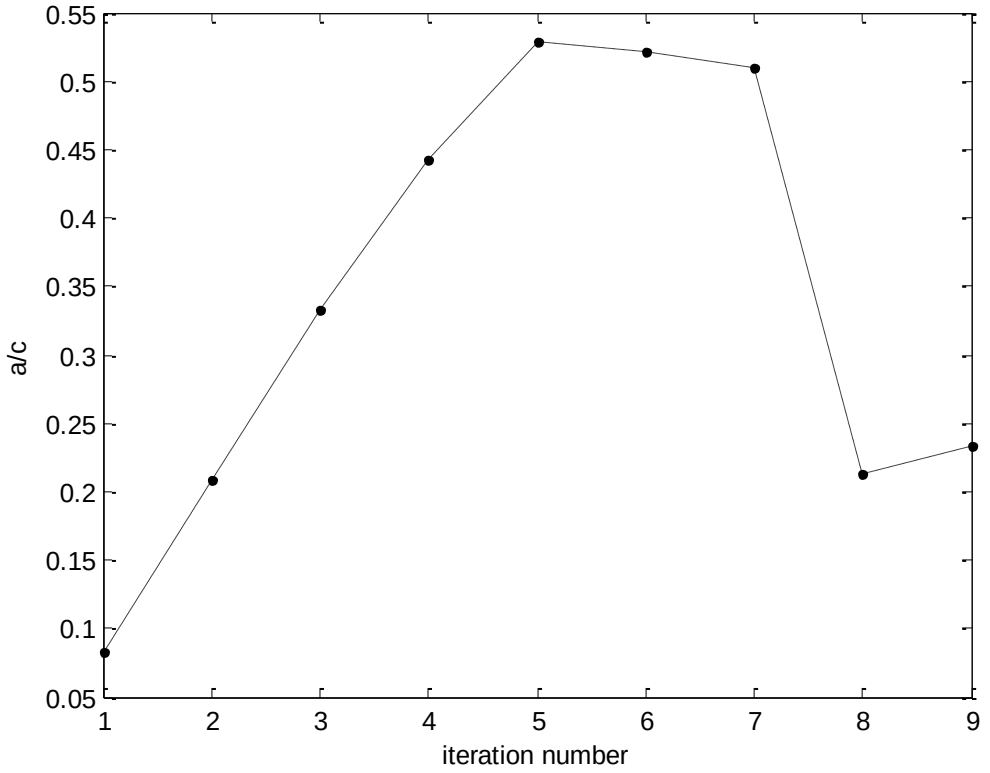

Figure 4.23 (b) Variation of a/c ratio as a function of iteration number

a = 3a, c = 3c and a/c = 1/5

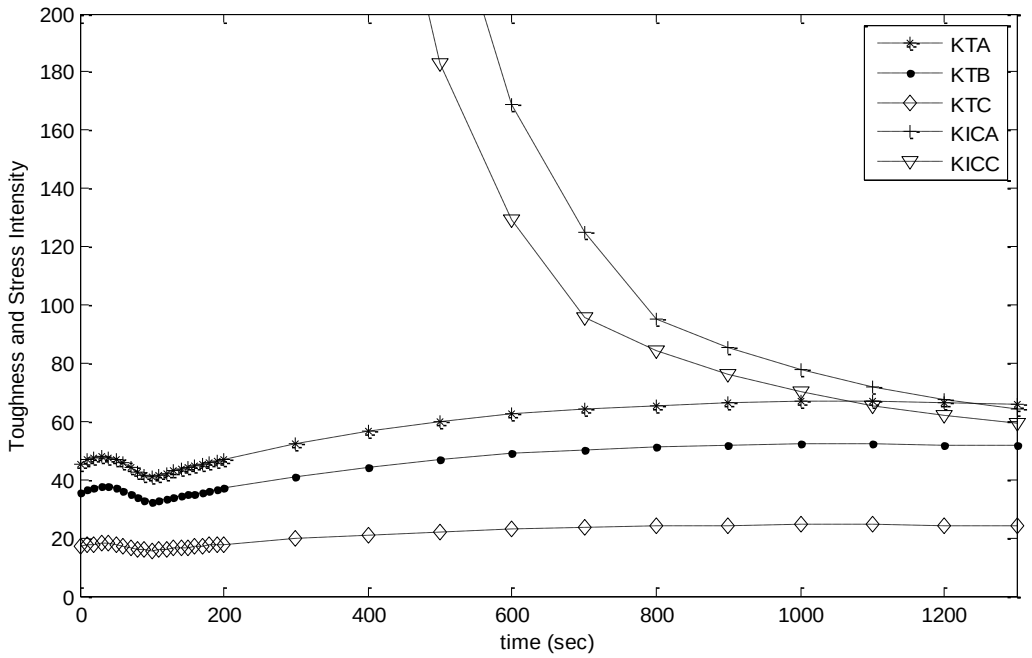

Figure 4.24 Variation of stress intensity and fracture toughness values as a function of time

For the first 1300 seconds the results are similar to the other ones. But when it comes to 1300th second, crack begins to propagate. To see the propagation arrest values at points a and c are given on below graph.

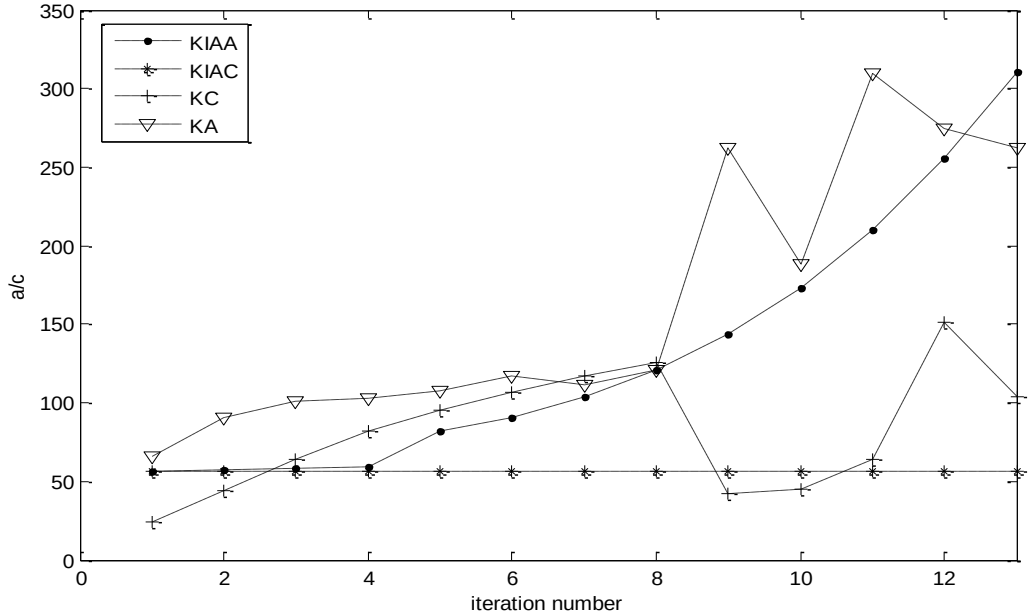

Figure 4.24 (a) Stress intensity and fracture toughness values as a function of iteration number

And the a/c values vs iteration number graph is as below:

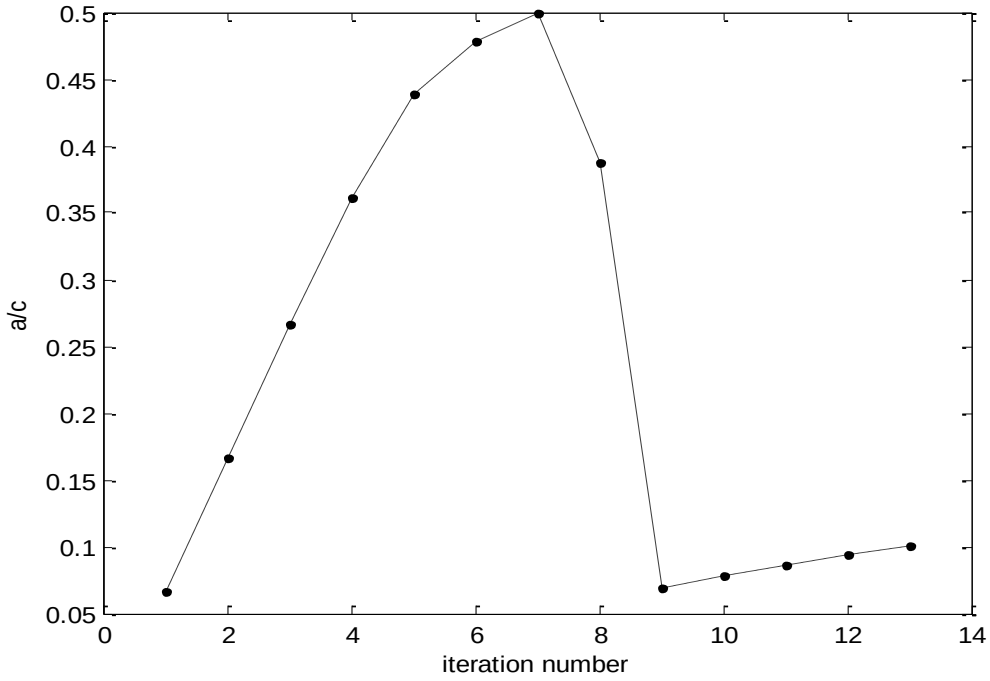

Figure 4.24 (b) Variation of a/c ratio as a function of iteration number

a = 4a, c = 4c and a/c = 1

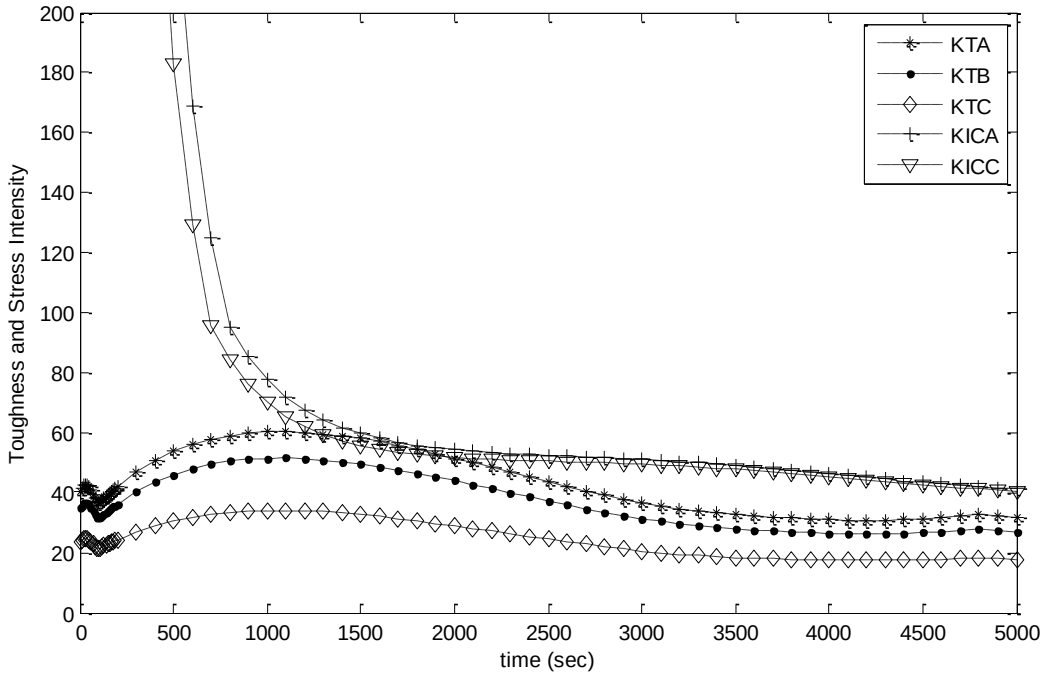

Figure 4.25 Variation of stress intensity and fracture toughness values as a function of time

a = 4a, c = 4c and a/c = ½

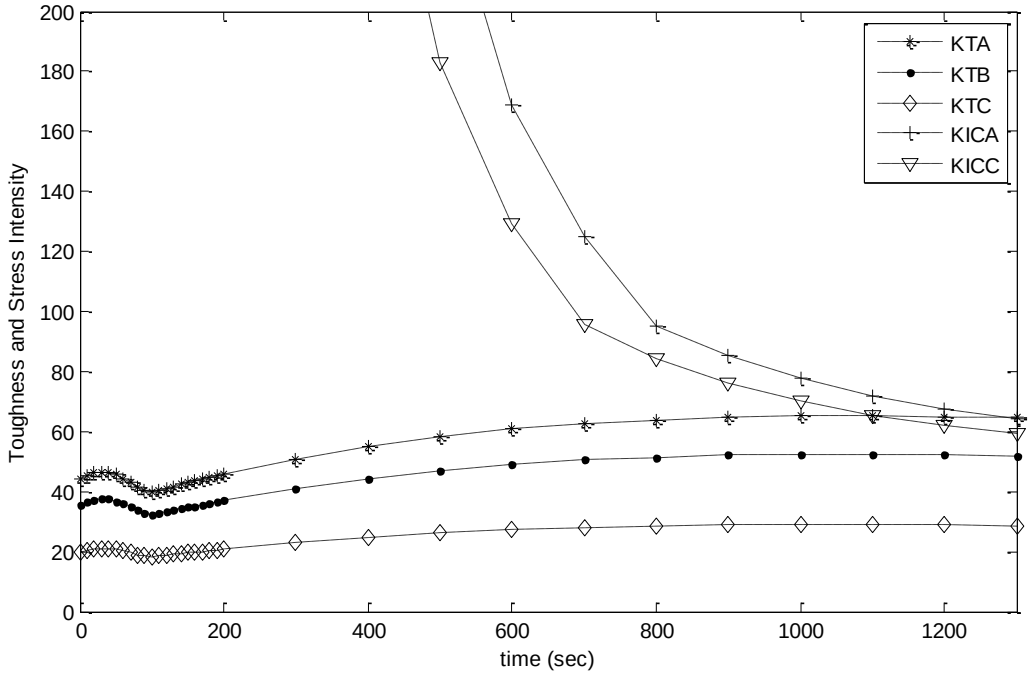

Figure 4.26 Variation of stress intensity and fracture toughness values as a function of time

For the first 1300 seconds fracture toughness values are higher than stress intensity factors. But when it comes to 1300th second, crack begins to propagate. To see if the crack arrests or not, fracture toughness for crack arrest values at points a and c are compared on Figure 4.26 (a).

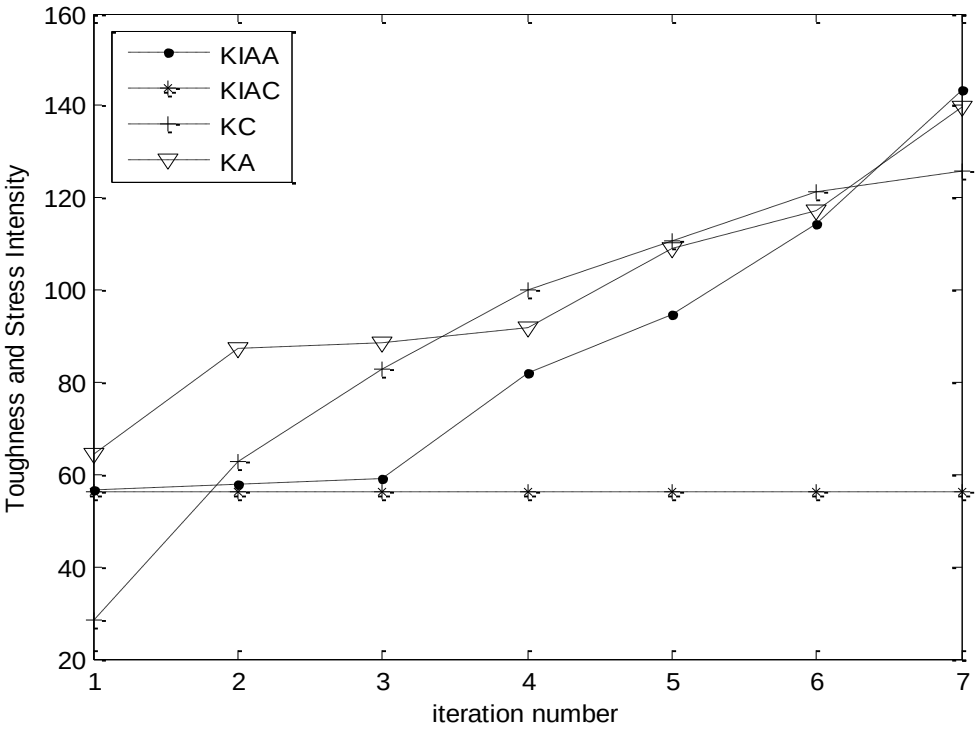

Figure 4.26 (a) Stress intensity and fracture toughness values as a function of iteration number

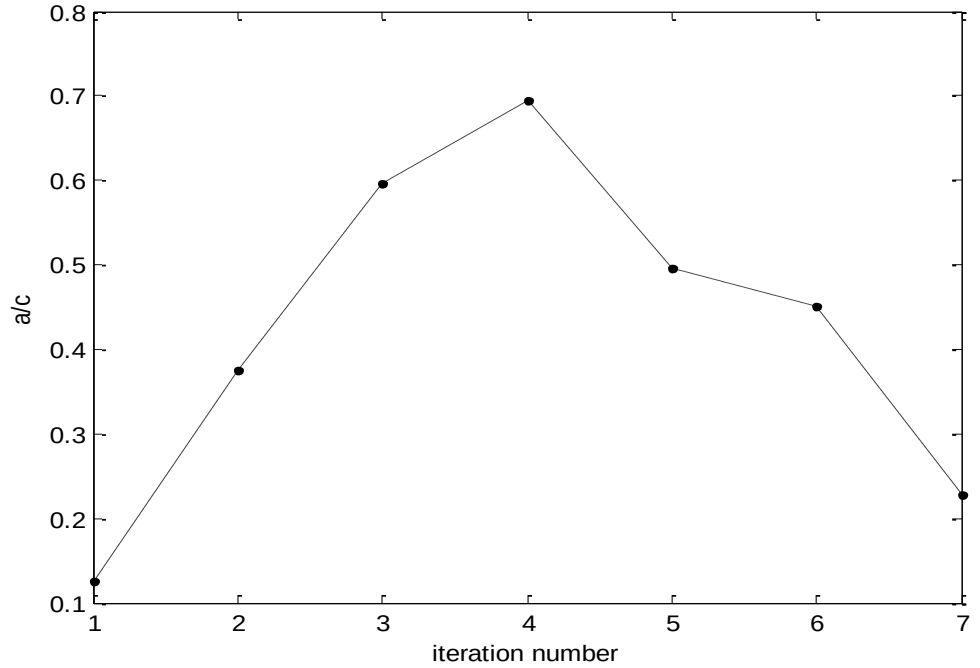

Figure 4.26 (b) Variation of a/c ratio as a function of iteration number

a = 4a, c = 4c and a/c = 1/3

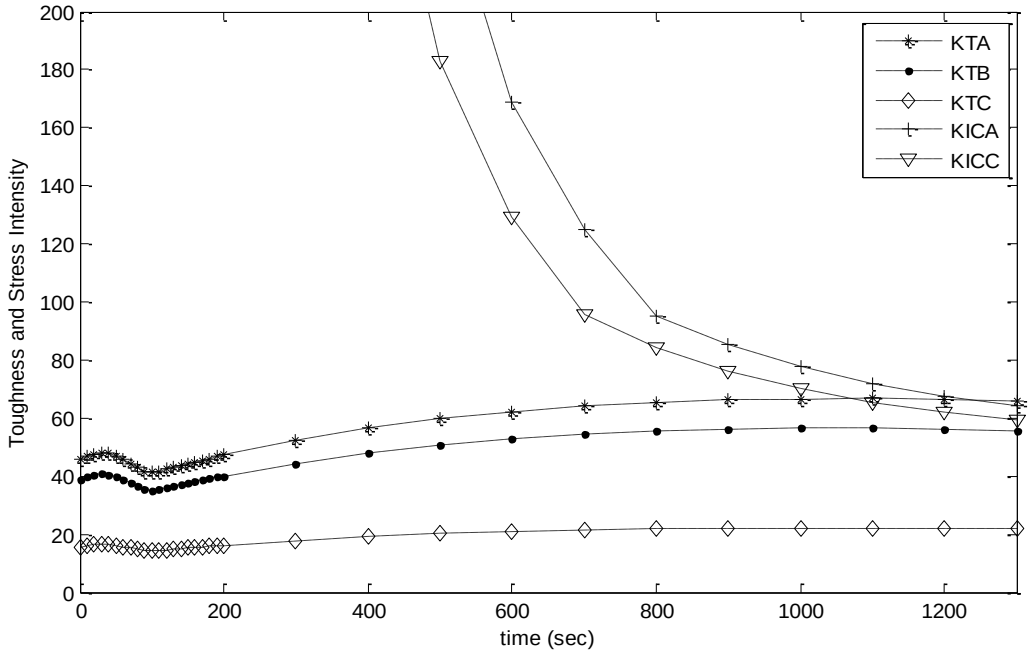

Figure 4.27 Variation of stress intensity and fracture toughness values as a function of time

For the first 1300 seconds the results are similar to the other ones. But when it comes to 1300th second, crack begins to propagate.

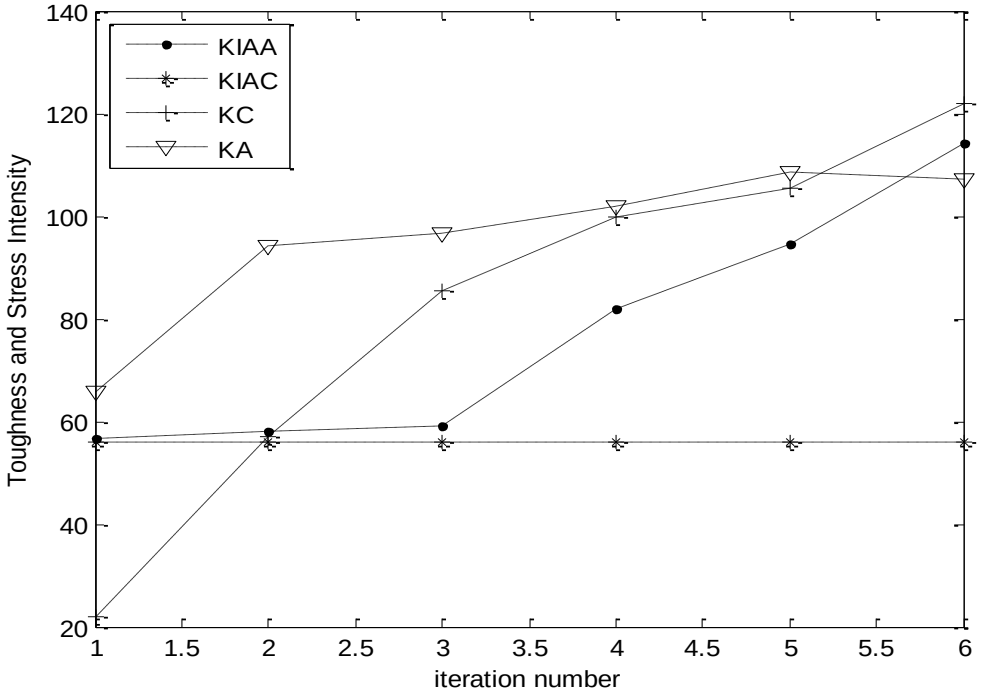

Figure 4.27 (a) Stress intensity and fracture toughness values as a function of iteration number

And the a/c values vs iteration number graph is as below:

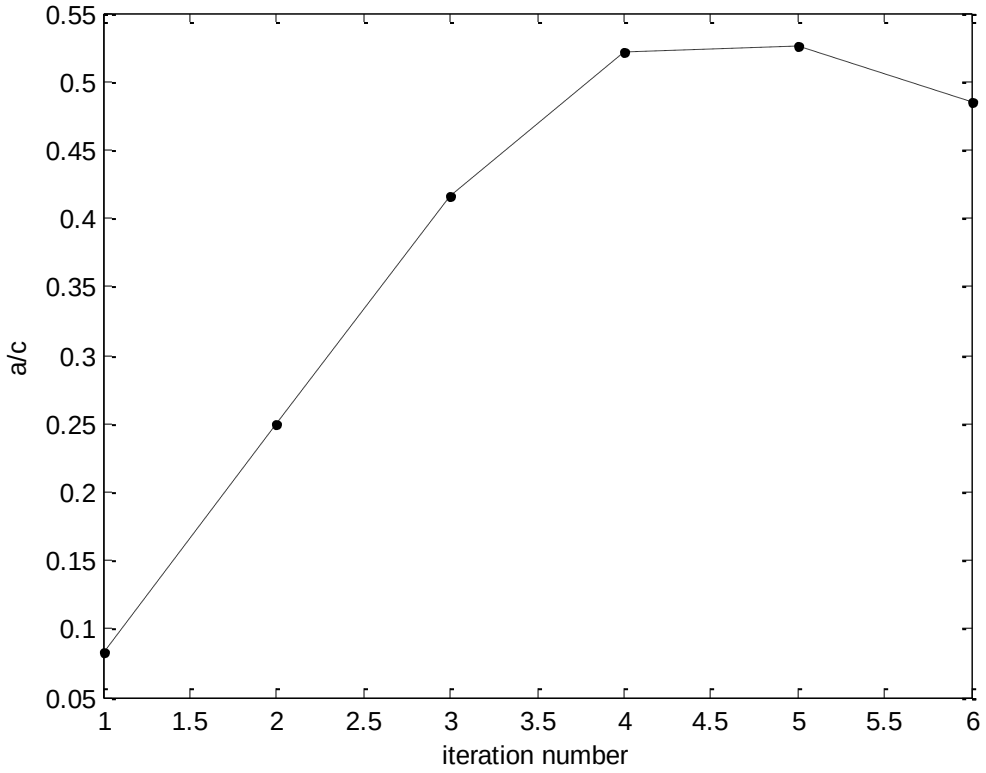

Figure 4.27 (b) Variation of a/c ratio as a function of iteration number

a = 4a, c = 4c and a/c = ¼

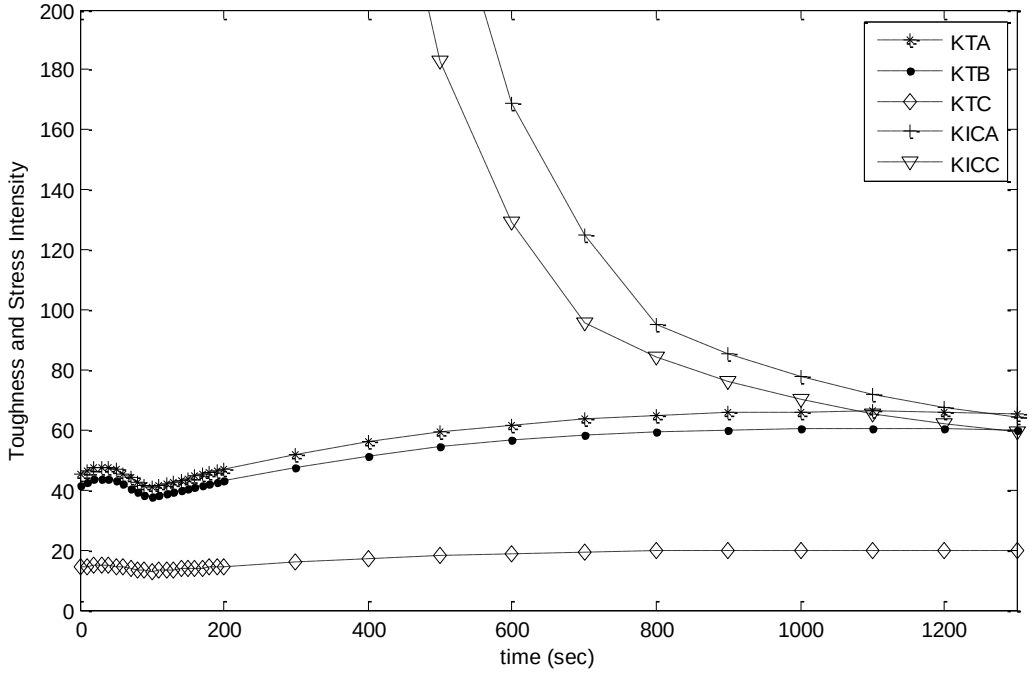

Figure 4.28 Variation of stress intensity and fracture toughness values as a function of time

For the first 1300 seconds the results are similar to the other ones. But when it comes to 1300th second, crack begins to propagate and fracture toughness for crack arrest are given on Figure 4.28 (a).

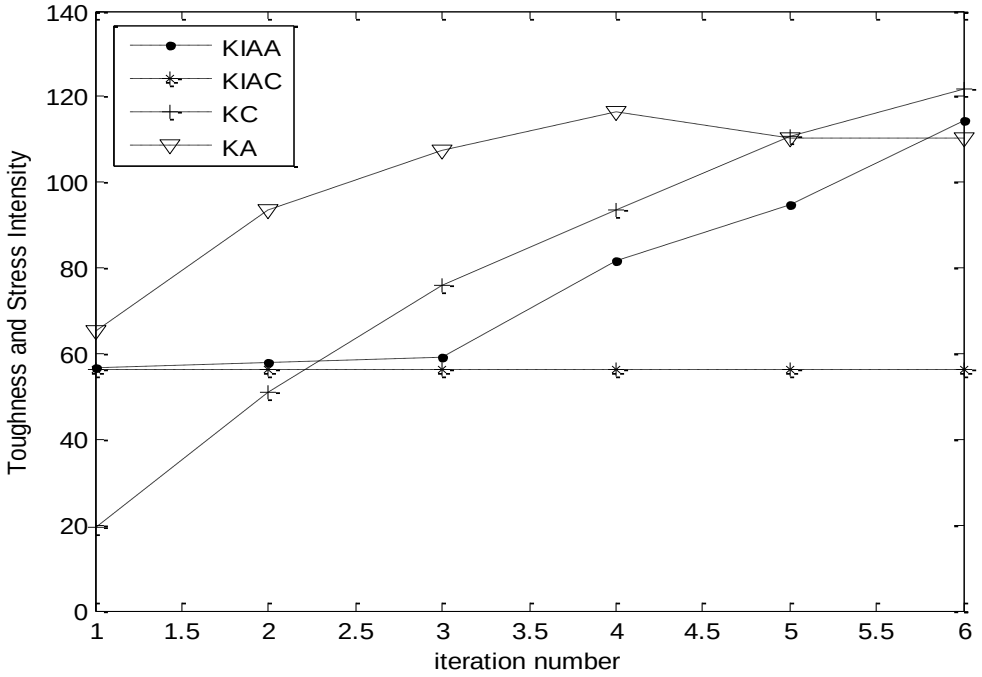

Figure 4.28 (a) Stress intensity and fracture toughness values as a function of iteration number

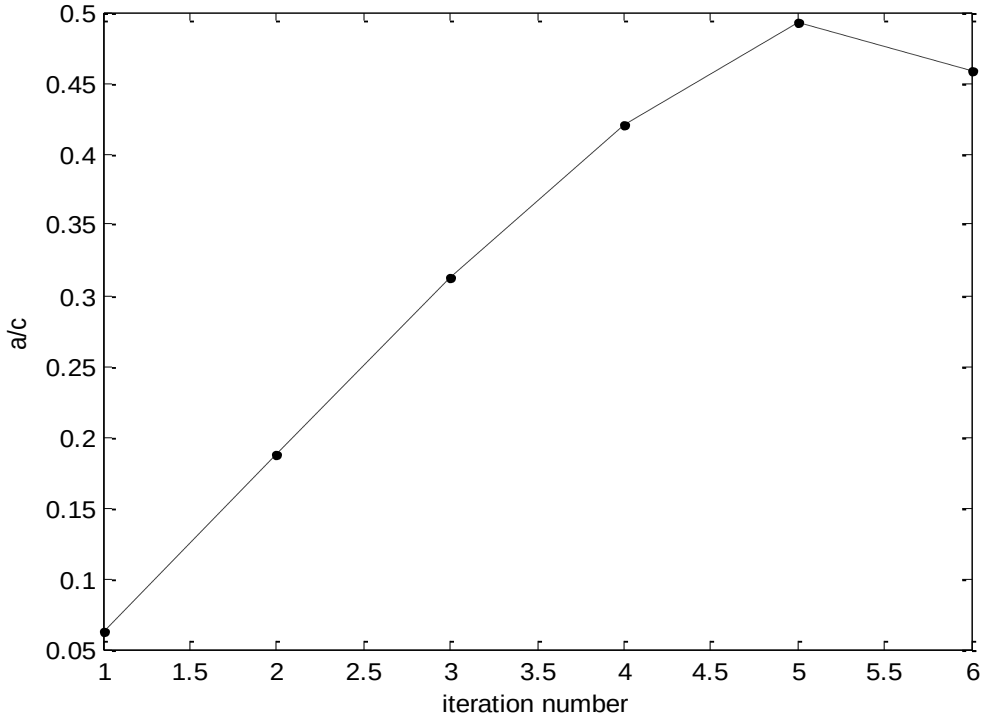

Figure 4.28 (b) Variation of a/c ratio as a function of iteration number

a = 4a, c = 4c and a/c = 1/5

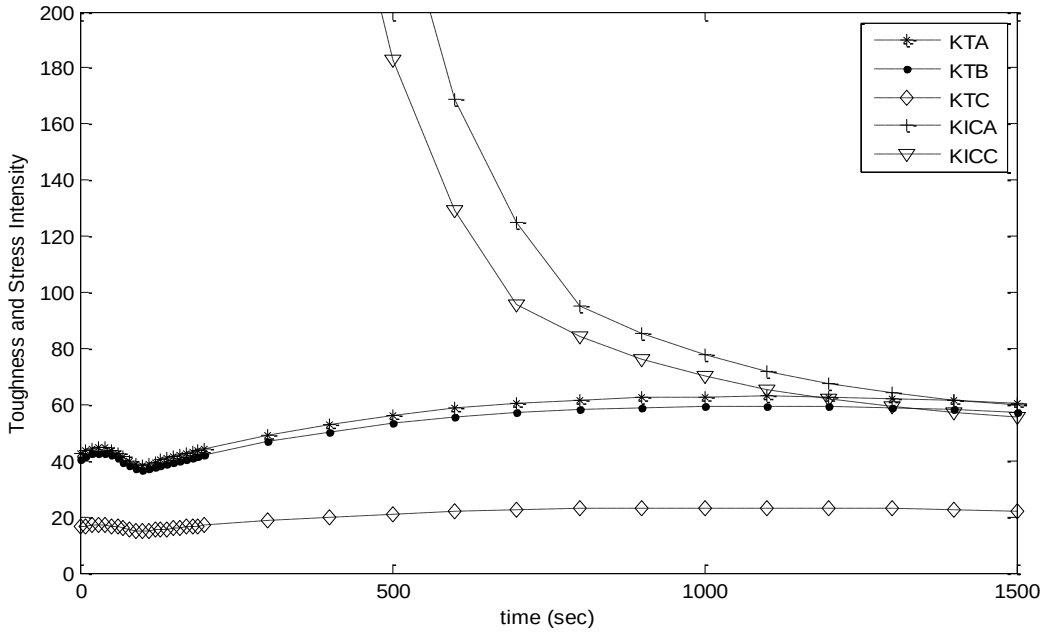

Figure 4.29 Variation of stress intensity and fracture toughness values as a function of time

For the first 1500 seconds the results are similar to the other ones. But when it comes to 1500th second, crack begins to propagate. To see the propagation arrest values at points a and c are given on below graph.

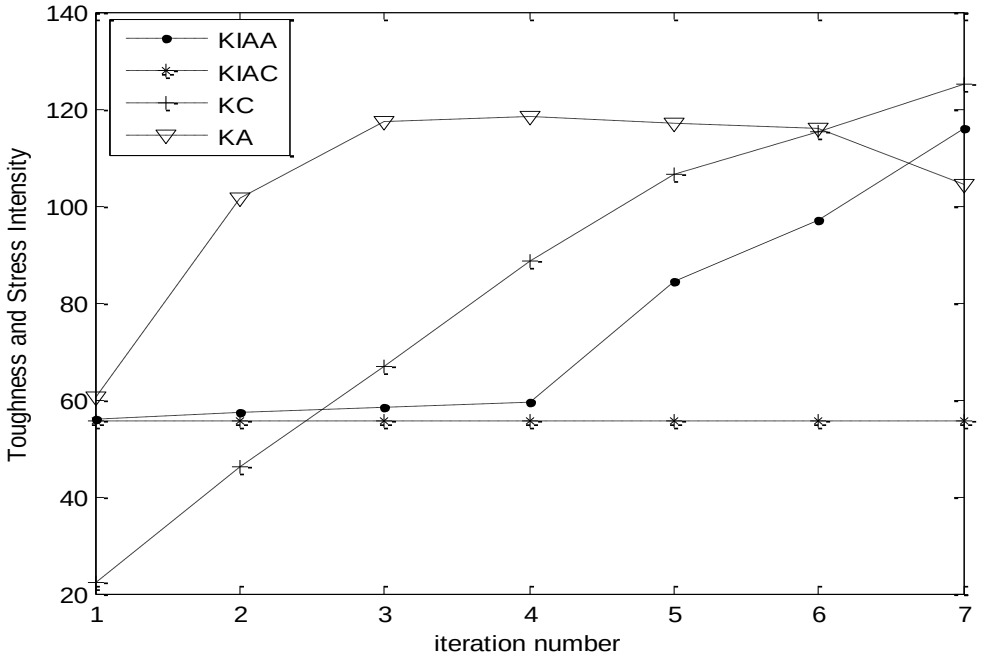

Figure 4.29 (a) Stress intensity and fracture toughness values as a function of iteration number

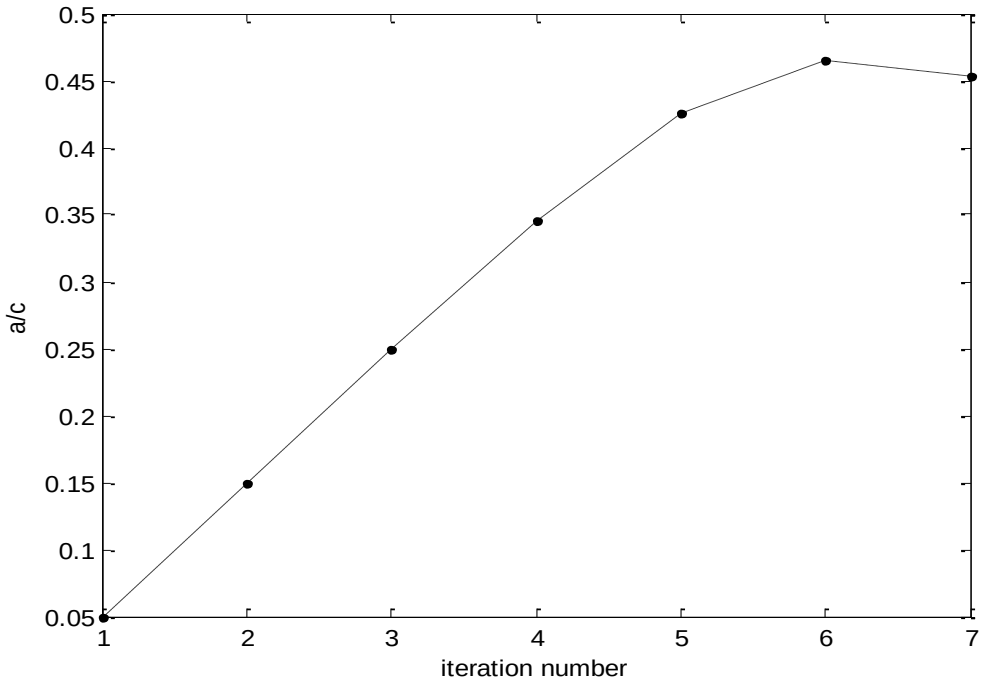

Figure 4.29 (b) Variation of a/c ratio as a function of iteration number

To summarize; the results of the analysis done for crack propagation for different cases of crack size and depth to length aspect ratio values are given in below tables.

Table 4.2 Results for crack sizes obtained from Marshall Distribution

a (cm)	a/c	Arrest	propagate
0.039	1	✓	
0.044	1	✓	
0.134	1	✓	
0.252	1	✓	
0.357	1	✓	
0.445	1	✓	
0.522	1	✓	

Table 4.3 Results for the biggest crack size for different a/c values

a (cm)	a/c	Arrest	propagate
0.522	1	✓	
0.522	½	✓	
0.522	1/3	✓	
0.522	¼	✓	
0.522	1/5		✓

Table 4.4 Results for a=2a, c=2c for different a/c values

a (cm)	a/c	Arrest	propagate
2a	1	✓	
2a	½	✓	
2a	1/3		✓
2a	¼		✓
2a	1/5		✓

Table 4.5 Results for a=3a, c=3c for different a/c values

a (cm)	a/c	Arrest	propagate
3a	1	✓	
3a	½		✓
3a	1/3		✓
3a	¼		✓
3a	1/5		✓

Table 4.6 Results for a=4a, c=4c for different a/c values

a (cm)	a/c	Arrest	propagate
4a	1	✓	
4a	½		✓
4a	1/3		✓
4a	¼		✓
4a	1/5		✓

As observed from the analysis, increasing crack size results in more dangerous situations on pressure vessel which means crack size has an important role in failure. According to pressure and temperature distributions, the stress intensity and fracture toughness values are obtained in the analysis and in Table 4.7 the cases that the crack propagates are listed.

Table 4.7 Temperature values at the time of propagation on crack tip points

		a/c	Time (sec)	Temp@c (^{0}C)	Temp@a (^{0}C)
a	C	1/5	1500	125.53	84.18
2a	2c	1/3	1400	138.45	87.83
		1/4	1300	159.74	92.18
		1/5	1300	174.30	92.18
3a	3c	1/2	1400	138.45	87.83
		1/3	1400	161.15	87.83
		1/4	1300	187.77	92.18
		1/5	1300	205.86	92.18
4a	4c	1/2	1300	159.74	92.18
		1/3	1300	187.76	92.18
		¼	1300	211.34	92.18
		1/5	1300	218.81	92.18

Temperature values increase as a/c values decreases. And as expected, temperature values are higher on pressure vessel's inner surface. When crack is extended, the propagation occurs earlier. These are the cases in which the crack cannot be arrested.

5. CONCLUSION AND RECOMMENDATIONS

In this study to calculate stress intensity factor of cracks in PWR pressure vessel, finite elements method was used. The analyses performed in this study are for SBLOCA which is basically a pressure and temperature transient. Temperature and pressure distributions are taken from an earlier SBLOCA simulation [3]. In SBLOCA the most important parameters that affect propagation are temperature and pressure distributions. Therefore firstly temperature gradient is obtained as a function of time and position by thermal analysis. Using temperature from thermal analysis and pressure values of a small break loss of coolant accident [3] and initial crack size obtained from Marshall flaw size distribution, copper and nickel contents of steel, initial reference temperature of the nil-ductility transition, fluence factor [3,8] as inputs to the code, stress intensity factor and fracture toughness for crack initiation and arrest values are obtained and compared to observe crack propagation.

For seven different crack sizes derived from Marshall distribution, the crack does not propagate. Even if the crack size gets bigger, the crack becomes more dangerous and may cause failure. For the biggest crack size obtained, new analyses are done for four different a/c values. And crack propagation occurs for the value of a/c=1/5. Then the crack is extended by multiplying a and c values. The propagation occurs for 2 times extended crack for a/c=1/3 value. When the crack is more extended, it starts to propagate earlier as expected. For 3 and 4 times extended crack, crack begins to propagate on the early steps of analysis.

Crack propagation is analyzed as a function of initial crack size. This study includes the effects of crack size and crack depth to crack length ratios to the crack propagation.

The presence of a crack on pressure vessel in the sizes obtained according to Marshall distribution has a very small probability in real life. Although these are the most dangerous cases for a crack size on vessel, it is observed that the propagation occurs just for a few cases. This shows us the reliability and the safety of the pressure vessels.

For future studies, crack may be assumed in the top or bottom part of the pressure vessel. As a result of chemical reactions on the upper part of the vessel, stress intensity is higher and the high stress in the bottom part will also cause higher stress intensity values which may be another case to be observed. In this analysis semi elliptical crack is assumed. For other crack shapes same analyses may be done.

6. REFERENCES

[1] Yıldırım B., Dag S., Erdoğan F., 2005, Three Dimensional Fracture Analysis of FGM Coatings Under Thermomechanical Loading, International Journal of Fracture, 132, 369-395.

[2] Hee Dong Kim, Development of CALF for Thermal and Failure Analysis of RPV Lower Head, Korea Atomic Energy Research Institute, Taejon, Korea

[3] Çolak Ü., Özdere O., 2001, Comparative Analysis of Pressure Vessel Integrity for Various LOCA Conditions, Journal of Nuclear Materials 297, 271-278.

[4] Jouniaux-Corriger Y., Izard J.P., Giles P., 2007, Three Dimensional Fracture Analysis of the Reactor Pressure Vessel Inlet Nozzle Under Pressurized Thermal Shock, Transactions, G02/2.

[5] Lewis E.E., 1977, Nuclear Power Reactor Safety, The Technological Institute Northwestern University, 368-380.

[6] Özdere O., 2000, Deterministic and Probabilistic Analysis of Pressure Vessel Under Pressurized Thermal Shock, A Thesis of Master of Science in Nuclear Engineering Department.

[7] Mukhopadhyay N.K., Pavan Kumar T.V., Chattopadhyay J., Dutta B.K., 1998, Deterministic Assessment of Reactor Pressure Vessel Integrity Under Pressurized Thermal Shock, Pressure Vessels and Piping, 75, 1055-1064.

[8] Simonen A., Johnson K.I., 1986, VISA II, A Computer Code for Predicting the Probability of Reactor Pressure Vessel Failure, Nureg/CR-4/PNL-5775.

[9] Moinereau D., Bezdikian G., Faidy C., 2001, Methodology for the Pressurized Thermal Shock Evaluation: Recent Improvements in French RPV PTS assessment, Pressure Vessel and Piping, 78, 69-83.

[10] EricksonKirk M., Junge M., 2007, Technical Basis for Revision of the Pressurized Thermal Shock (PTS) Screening Limit in the PTS Rule (10 CFR 50.61), NUREG-1806, Vol. 1.

[11] Shib-Jung Chang, 1995, The method of Life Extension For the High Flux Isotope Reactor Vessel, Oak Ridge National Laboratory, Tennesse.

[12] U.S. Nuclear Regulatory Commission Regulatory Guide 1.99, Revision 2

[13] Chawla D.S., Bhate S.R., Kushwaha H.S.,, 2000, Numerical simulation of crack growth and arrest in a vessel under pressure thermal shock, International Journal of Pressure Vessels and Piping, 77, 261-271.

[14] Doe Jeong Lee, Sung Quun Zee, Nuclear Power Reactor Technology, Module 1-2.
[15] http://www.nrc.gov/reading-rm/doc-collections